0026-895X/09/7503-713–728$20.00
MOLECULAR PHARMACOLOGY
Copyright © 2009 The American Society for Pharmacology and Experimental Therapeutics
Mol Pharmacol 75:713–728, 2009

Vol. 75, No. 3
50765/3445511
Printed in U.S.A.

Facilitatory Interplay in α_{1a} and β_2 Adrenoceptor Function Reveals a Non-G_q Signaling Mode: Implications for Diversification of Intracellular Signal Transduction[S]

Alicja J. Copik, Cynthia Ma, Alan Kosaka, Sunil Sahdeo, Andy Trane, Hoangdung Ho, Paul S. Dietrich, Helen Yu, Anthony P. D. W. Ford, Donald Button, and Marcos E. Milla

Inflammation Discovery (A.J.C., C.M., S.S., A.T., A.P.D.W.F., D.B., M.E.M.) and Discovery Technologies (A.K., H.H., P.S.D., H.Y.), Roche Palo Alto, Palo Alto, California

Received July 24, 2008; accepted December 24, 2008

ABSTRACT

Agonist occupied α_1-adrenoceptors (α_1-ARs) engage several signaling pathways, including phosphatidylinositol hydrolysis, calcium mobilization, arachidonic acid release, mitogen-activated protein (MAP) kinase activation, and cAMP accumulation. The natural agonist norepinephrine (NE) activates with variable affinity and intrinsic efficacy all adrenoceptors, and in cells that coexpress α_1- and β-AR subtypes, such as cardiomyocytes, this leads to coactivation of multiple downstream pathways. This may result in pathway cross-talk with significant consequences to heart physiology and pathologic state. To dissect signaling components involved specifically in α_{1A}- and β_2-AR signal interplay, we have developed a recombinant model system that mimics the levels of receptor expression observed in native cells. We followed intracellular Ca^{2+} mobilization to monitor in real time the activation of both G_q and G_s pathways. We found that coactivation of α_{1A}- and β_2-AR by the nonselective agonist NE or via a combination of the highly selective α_{1A}-AR agonist A61603 and the β-selective agonist isoproterenol led to increases in Ca^{2+} influx from the extracellular compartment relative to stimulation with A61603 alone, with no effect on the associated transient release of Ca^{2+} from intracellular stores. This effect became more evident upon examination of an α_{1A}-AR variant exhibiting a partial defect in coupling to G_q, and we attribute it to potentiation of a non G_q-pathway, uncovered by application of a combination of xestospongin C, an endoplasmic reticulum inositol 1,4,5-triphosphate receptor blocker, and 2-aminoethoxydiphenyl borate, a nonselective store-operated Ca^{2+} entry channel blocker. We also found that stimulation with A61603 of a second α_{1A}-AR variant entirely unable to signal induced no Ca^{2+} unless β_2-AR was concomitantly activated. These results may be accounted for by the presence of α_{1A}/β_2-AR heterodimers or alternatively by specific adrenoceptor signal cross-talk resulting in distinct pharmacological behavior. Finally, our findings provide a new conceptual framework to rationalize outcomes from clinical studies targeting α- and β-adrenoceptors.

Given the diversity of physiological processes controlled by G protein-coupled receptors (GPCRs or 7-transmembrane receptors) and the large number of receptors from this family coexpressed in different tissues, it comes as no surprise that linear signal transduction models cannot accommodate the many observed pharmacological outcomes that follow receptor activation. It is generally understood that intracellular signal transduction pathways stemming from the activation of GPCRs interact significantly to add layers of complexity to their regulation, sometimes leading to novel signaling modes (Cordeaux and Hill, 2002). In addition, many receptors have been shown to couple to more than one G protein, and also initiate G protein-independent signaling upon stimulation (for review, see Gilchrist, 2007; Violin and Lefkowitz, 2007).

Such GPCR signaling cross-talk can be initiated at the

Article, publication date, and citation information can be found at http://molpharm.aspetjournals.org.
doi:10.1124/mol.108.050765.
[S] The online version of this article (available at http://molpharm.aspetjournals.org) contains supplemental material.

ABBREVIATIONS: GPCR, G protein-coupled receptor; 2-APB, 2-aminoethoxydiphenyl borate; A61603, *N*-[5-(4,5-dihydro-1*H*-imidazol-2-yl)-2-hydroxy-5,6,7,8-tetrahydro-naphthalen-1-yl]methanesulfonamide hydrobromide; AR, adrenoceptor; CYP, cyanopindolol; EBNA, Epstein-Barr virus nuclear antigen; ERK, extracellular signal-regulated kinase; FRET, Förster resonance energy transfer; H89, *N*-[2-(4-bromocinnamylamino)ethyl]-5-isoquinoline; HEK, human embryonic kidney; ICI 118551, erythro-DL-1-(7-methylindan-4-yloxy)-3-isopropylaminobutan-2-ol; ICL-3, third intracellular loop; IP, inositol phosphate; IP_3, inositol 1,4,5-triphosphate; IP_3R, inositol 1,4,5-triphosphate receptor; MDL12,330A, *cis*-*N*-(2-phenylcyclopentyl)-azacyclotridec-1-en-2-amine hydrochloride; NaBu, sodium butyrate; NE, norepinephrine; NECA, 5′-*N*-ethylcarboxamidoadenosine; PKA, cAMP-dependent protein kinase; RS100329, 5-methyl-3-[3-[4-[2-(2,2,2,-trifluoroethoxy)phenyl]-1-piperazinyl]propyl]-2,4-(1*H*)-pyrimidinedione; SOC, store-operated Ca^{2+}; TCM, tetracysteine motif (CCPGCC).

level of the receptor, via formation of heterodimers, or result from downstream integration of signals derived from other receptors with no physical association. For the adrenoceptor (AR) family, formation of functional homo and heterodimers is emerging as a common theme, and its importance has been documented with multiple pharmacological observations (for review, see Prinster et al., 2005). Heterodimerization of α_{1D}-AR with either β_2-AR or α_{1B}-AR seems essential for its biogenesis and cell surface expression. α_{1D}/α_{1B}-AR heterodimers also exhibit distinct ligand pharmacology and show enhanced agonist mediated activity relative to either subtype alone. Many other heteroreceptor couplings have been reported to affect such aspects of receptor function as pharmacological behavior, internalization and desensitization, and differential signal transduction pathways. They include α_{1A}/α_{1B}-, β_1/α_{2A}- and β_2/β_1-AR (for review, see Prinster et al., 2005). Formation of heterodimers is not limited to within the adrenoceptor family members: adrenoceptors can also dimerize with opioid, muscarinic, histaminic, and olfactory GPCRs (for review, see Prinster et al., 2005).

Signaling cross-talk may also result from the regulation of receptor function by accessory proteins or from the modification of the signaling properties of effector molecules by other elements of the activated pathway. Such interactions have been observed to increase or cross-inhibit responses, recruit cytoskeletal proteins, modulate channel activity, or down-regulate receptor expression (reviewed in Hur and Kim, 2002; Werry et al., 2003). Pathway cross-talk has been introduced to describe inconsistent behavior of certain pharmacological agents such as β- and α-AR agonists. Indeed, multiple studies have focused on the cardiac AR subtypes, particularly on interactions of α_1- and β_1-AR agonists in the regulation of cardiac contractility and pace (reviewed in Dzimiri, 2002). Much less is known with regard to interactions between α_1 and β_2-ARs, yet intriguing studies in aging and failing human hearts showed up-regulation of the expression of α_{1A}-AR, with concomitant down-regulation of the β_1-AR, whereas β_2-AR expression levels remained unchanged (Woodcock et al., 2008). The resulting changes in the α_1/β_2- versus β_1-AR ratios suggest a crucial role for α_1-AR in inotropic signaling and cytoprotection in the failing heart (Skomedal et al., 1997; Huang et al., 2007; Woodcock et al., 2008). At present, a framework for understanding the interplay between α_1 and β_2-adrenoceptors in intracellular signaling is lacking. Coexpression of α_{1A}- and β_2-ARs in a model system was used for the functional dissection of cross-talk between those receptors, and in particular, one that allowed expression densities more closely matched to those seen in cardiomyocytes.

As part of our efforts to develop a SAR for selective α_{1A}-AR agonists, we have identified receptor variants (at the level of the 3rd intracellular loop) that are defective for signaling through their canonical pathways. By taking advantage of the endogenous expression of β_2-AR in HEK-293 cells, we have developed a transient expression model system for α_{1A}-AR in which this receptor is expressed at relatively low levels comparable with those observed in native cells and tissues. We have used this system to monitor the kinetics of responses occurring within seconds upon agonist stimulation of α_{1A}, β_2, or both adrenoceptors. Onset of calcium signals resulting from G_q-phospholipase C-inositol 1,4,5-triphosphate receptor (IP_3R) coupling is much faster relative to G_s-mediated responses, probably because of the previously reported lag time for cAMP accumulation (Lohse et al., 2008a). This temporal resolution of signals has allowed us to monitor, in real-time, G_q and G_s signals converging on Ca^{2+} mobilization. We have also used this model to study signaling-defective α_{1A}-AR variants and detected strong potentiation of Ca^{2+} mobilization on costimulation of α_{1A} and β_2 adrenoceptors. Furthermore, the reconstitution of α_{1A}-AR function by coexpression with β_2-AR suggests a direct interaction of these two receptors or convergence of downstream signaling pathways. These data may greatly help our understanding of the pathogenesis and progression of heart failure and may suggest approaches for therapeutic intervention.

Materials and Methods

Materials and Reagents. Reagents were purchased from the following commercial suppliers: A61603, xamoterol, procaterol, and fenoterol from Tocris (Ellisville, MO); norepinephrine, prazosin, phentolamine, ICI 118551, atenolol, salbutamol, propranolol, probenecid, bovine serum albumin, and glucose from Sigma-Aldrich (St. Louis, MO); isoproterenol and oxymetazoline from MP Biomedicals (Irvine, CA), sodium butyrate from Alfa Aesar (Ward Hill, MA); 2-APB from Calbiochem (San Diego, CA); xestospongin C from Cayman Chemical (Ann Arbor, MI); HEPES, Hanks' buffered salt solution, and Fluo3-acetoxymethyl ester from Invitrogen (Carlsbad, CA). [^{3}H]Prazosin and ^{125}I-CYP were purchased from PerkinElmer Life and Analytical Sciences (Waltham, MA). Crude membranes were prepared from transduced or transfected HEK-293/EBNA cells as described previously (Waugh et al., 1999) with one modification: cells were resuspended in the lysis buffer without sucrose and broken using a Polytron homogenizer (three 30-s pulses; Kinematica, Lucerne, Switzerland).

Constructs. The wild-type α_{1A}-AR codon altered sequence was based on α_{1A}-AR isoform 1 (GenBank NM_000680). The full-length gene was synthesized (DNA 2.0, Menlo Park, CA) with an N-terminal hemagglutinin tag (YPYDVPDYA) inserted between codons for Val2 and Gly3, unique 5′-SacII and 3′-XhoI restriction sites flanking the region of the I3 loop to exchange CCPGCC (tetracysteine motif, TCM) I3 loop variants, a C-terminal 8× His tag followed by a Flag tag, and additional spacer amino acids followed by a stop codon (GS**HHHHHHHH**GS**DYKDDDDK**GGSTG-stop; bold segments indicate the 8× His and Flag tags, respectively; additional residues indicate spacer amino acids). This wild-type tagged α_{1A}-AR gene was synthesized in a Gateway-compatible plasmid and transferred by LR Clonase reaction (Invitrogen) into a high-copy Gateway modified BacMam expression vector derived from pTriEx3 (EMD Biosciences, San Diego, CA).

For the insertion variant Ins_α_{1A}-AR, the TCM was placed between codons for Gly244 and Gly245. For the substitution variant Sub_α_{1A}-AR, the TCM was replaced for the sequence DSEQVT233. Both variants were created by synthesizing I3 loop fragments containing the TCM CCPGCC flanked by SacII and XhoI restriction sites. To generate these variants, a codon-altered wild-type α_{1A}-AR Gateway-compatible construct was digested with SacII and XhoI and replaced with the insertion or substitution variant SacII-XhoI synthetic I3 loop fragment. These variants were then transferred by LR Clonase into the high-copy Gateway-modified pTriEx3 expression vector.

The pTriEx recombinants were cotransfected along with the BD BaculoGold linearized baculovirus DNA (BD Biosciences, San Jose, CA) into Sf9 insect cells using Insect Gene Juice (Novagen, Madison, WI) transfection reagent. Cells were incubated at 27°C, with shaking for 7 days to allow generation of recombinant baculovirus (vTriEx). The virus containing supernatant was then harvested, and infections of larger volume Sf9 cultures were performed to amplify virus stocks. Viruses were titered and expression of receptor was verified by Western blot, radioligand binding, and antibody staining.

Cell Culture and Transient Transductions. Cell-based experiments were performed using suspension-adapted HEK-293/EBNA cells. These cells were grown in Free Style 293 media (Invitrogen) and maintained in a humidified incubator at 37°C in 7% CO_2 with constant shaking at 150 rpm. Before experiments, cells were transduced with baculoviral strains harboring α_{1A}-AR, aldehyde oxidase, or viral medium (untransduced control). This was performed by incubating the cells with virus (multiplicity of infection, 100–150) for 3 to 4 h followed by exchange into fresh growth medium supplemented with 4 mM sodium butyrate (NaBu). Cells were grown for another 14 to 18 h, then examined for agonist-evoked responses in both intracellular Ca^{2+} mobilization and inositol monophosphate (IP) accumulation assays. Surface receptor density was determined by flow cytometry employing immunofluorescence labeling of the receptor's N-terminal hemagglutinin epitope tag and by radioligand binding using partially purified membranes.

Ca^{2+} Mobilization Fluorometric Imaging Plate Reader Assay. Virally transduced HEK-293/EBNA cells were resuspended in Hanks' balanced salt solution without Mg^{2+}, Ca^{2+}, and phenol red (Invitrogen), supplemented with 2 mM $CaCl_2$, 10 mM HEPES, pH 7.4, 2.5 mM probenecid, plus 1 g/liter glucose and 1 g/liter bovine serum albumin. Cells were then seeded in poly-D-lysine–coated 96-well black plates with transparent bottom (Costar; Corning Life Sciences, Acton, MA) at a density of 50,000 cells/well (0.1-ml volume). Cells were incubated for 1 h at 37°C after addition of 0.1 ml of buffer supplemented with 4 μM Fluo3-acetoxymethyl ester (1 mM stock solution prepared in 10% Pluronic F-127/dimethyl sulfoxide and diluted to 4 μM with loading buffer). Plates were then washed twice with 100 μl of buffer, and each well was refilled with 100 μl of assay buffer. Agonist-evoked Ca^{2+} mobilization was monitored via fluorometric imaging (MDS Analytical Technologies, Sunnyvale, CA). In experiments testing the effect of antagonist or inhibitor, 25 μl of buffer was removed from the washed cells, and 25 μl of vehicle or test compound was added back to the wells, followed by incubation for the indicated times (typically 5–30 min; see figure legends) before measurement of agonist-evoked responses. A baseline fluorescence measurement (excitation at 488 nm, emission at 510–570 nm) was obtained, and responses to agonist were observed after addition of 50 μl/well agonist solution. Fluorescence (F) was measured for 1.5 to 2 min at 1-s intervals. All data were normalized to baseline fluorescence (F_0) recorded 10 s before agonist addition and are represented as F/F_0, where $F/F_0 = (F - F_0)/F_0 + 1$ at each time point.

IP Accumulation Assay. Virally transduced HEK-293/EBNA cells were washed by centrifugation at 150*g* (8 min) and resuspended in the assay buffer (20 mM HEPES, 50 mM LiCl, 10 mM glucose, 1.8 mM $CaCl_2$, and 0.5 mM $MgSO_4$, in 1× Hanks' buffered salt solution) at a density of 10^7 cells/ml. Cells were dispensed in a 10-μl volume in a 384-well black polystyrene plate (Costar; Corning Life Sciences) at 10^5/well and incubated with 10 μl of antagonist or vehicle at room temperature. After 10 min, 10 μl of agonist solution was added; incubations with agonist were varied from 5 to 30 min and stopped by addition of lysis buffer. Total IP was quantified using a homogeneous immunoassay method with time-resolved FRET detection (IP-One; Cisbio International, Bedford, MA), according to the instructions provided by the supplier. Fluorescence emission of the donor (λ = 620 nm) and acceptor (λ = 665 nm) were measured using a PHERAstar plate reader (BMG Labtech, Durham, NC). Triplicate samples were analyzed per data point, and each experiment was performed independently at least two times.

Radioligand Binding Studies. Ligand binding affinity was determined using membranes prepared from HEK-293/EBNA cells virally transduced or transiently transfected with α_{1A}-AR constructs. [^{3}H]prazosin and ^{125}I-CYP were used as radioligands, and 100 μM phentolamine or 10 μM propranolol, respectively, was used as the nonradioactive competitor to determine nonspecific binding. For competition binding assays, unlabeled ligands (A61603, NE, and oxymetazoline) were used to compete [^{3}H]prazosin or ^{125}I-CYP binding. Reactions were set up in a 96-well polypropylene deep well block (Beckman-Coulter, Fullerton, CA) and initiated by the addition of 100 μl of membranes (5–40 μg of protein) to the mixture of radioligand and unlabeled competitor to give a final volume of 250 μl with buffer composition of 20 mM HEPES, 6 mM $MgCl_2$, and 1.4 mM EGTA, pH 7.4. The final concentrations of radioligands were 0.5 nM for [^{3}H]prazosin and 1 pM for ^{125}I-CYP. Plates were sealed with Parafilm (American National Can, Chicago, IL) and incubated for 90 min at 25°C. Reactions were terminated by rapid transfer to GF/B Unifilter-96 filter plates (PerkinElmer Life and Analytical Sciences) using a Packard Filtermate 196 Harvester (PerkinElmer Life and Analytical Sciences), followed by two 1-ml washes with ice-cold 50 mM HEPES buffer, pH 7.4. UniFilters were dried in a fume hood for at least 1 h, and their backs were sealed with backing tape. Fifty microliters of MicroScint-20 (PerkinElmer Life and Analytical Sciences) was added to each well, and the plates were sealed with TopSeal-A (PerkinElmer Life and Analytical Sciences). Filters were soaked overnight, and the radioactivity was counted using a Packard TopCount microplate scintillation counter (PerkinElmer Life and Analytical Sciences). IC_{50} values were estimated using the nonlinear least-squares fitting methods (Prism; GraphPad Software, San Diego, CA), and pK_i values were calculated according to the Cheng-Prusoff correction (Cheng and Prusoff, 1973).

Data Analysis. Experiments were performed multiple times and carried out in replicates (n indicated in figure legends). Graphs shown reflect either pooled or representative data (see figure legends). For dose-response analysis, results from Ca^{2+} mobilization experiments were plotted as peak F/F_0 versus agonist concentration and fitted to a sigmoidal dose-response equation using the Prism software package. For radioligand binding experiments, B_{max} values were calculated from maximum binding using the equation $B_{max} = (SB \cdot (IC_{50} + [L])/[L])$, where SB is the specific binding expressed in femtomoles per milligram of membrane protein and [L] is the ligand concentration.

Results

Identification of α_{1A}-ARs Displaying G Protein Coupling Defects. In generating probes to study GPCR conformational transitions that couple agonist binding to G protein activation via Förster resonance energy transfer (FRET), we prepared several mammalian cell expression constructs for fluorescent labeling, containing the arsenical-reactive TCM (CPGCC; Hoffmann et al., 2005) in the third intracellular loop (ICL-3) of the α_{1A}-AR, either as an insertion or a substitution. This strategy has been successfully applied to several receptors to observe ligand-induced conformational transitions leading to significant changes in the distance between the ICL-3 and the C terminus of the receptor, thus changing FRET from the fluorescent probes placed at these two positions (for review, see Lohse et al., 2008b). The exact placement of TCM within ICL-3 was aimed at avoiding any effect on G protein coupling. Thus, amino acid positions found to participate in G protein coupling, or binding to scaffolding proteins, were avoided (Cotecchia et al., 1990; Greasley et al., 2001). However, two of three variant receptors exhibited deficiencies in signaling. The insertion mutant Ins_α_{1A}-AR displayed a partial coupling defect, and the substitution mutant Sub_ α_{1A}-AR showed no functional coupling, as determined by their ability to produce IP in response to NE stimulation (Fig. 1, A–D). Treatment of cells expressing wild-type α_{1A}-AR with the α_{1A}-selective agonist A61603 or the native agonist NE induced similar levels of IP production at maximally effective agonist concentrations (Fig. 1A). In both cases, EC_{50} values were close to those previously reported for these agonists (NE, 0.9 μM; A61603, 0.04 μM; Table 1) (Ford

et al., 1997). Cells bearing the variant Ins_α_{1A}-AR also showed similar rates of IP formation in response to both NE and A61603, yet those rates were lower relative to the ones observed in cells transduced with wild-type_α_{1A}-AR, probably because of a decrease in signaling efficiency of that receptor variant (Fig. 1B). A modest decrease in potency was detected in these cells for both agonists (NE, EC_{50} = 4 μM; A61603, EC_{50} = 0.2 μM; Table 1). No IP accumulation was detected with the Sub_α_{1A}-AR variant in response to NE or A61603 (Fig. 1C). Finally, in untransduced HEK 293 cells, treatment with these agonists resulted in no IP accumulation (Fig. 1D). These results indicate a partially defective signaling phenotype for the insertion variant Ins_α_{1A} AR and complete impairment for the substitution variant Sub_α_{1A}-AR. However, Ins_α_{1A}-AR and Sub_ α_{1A}-AR showed near-wild-type binding properties for all ligands studied (Table 2), suggesting that their overall fold and structural stability is probably not affected by those modifications. Therefore, we considered these variants showing signaling defects to constitute useful tools for pharmacological studies aimed at dissecting the modes of signaling of α_{1A}-ARs through downstream intracellular pathways.

A System to Image Adrenoceptor Function Using a Ca^{2+} Measure. We studied these wild-type and mutant α_{1A}-AR baculovirus-delivered constructs based also on their ability to drive a fairly low level of surface receptor expression in most cells, as verified by antibody labeling and radioligand binding using crude membrane preparations (Table 2 and Supplemental Figure S1, A and B) compared with the stably transfected Chinese hamster ovary_α_{1A}-AR. Radioligand binding experiments indicate that expression levels were in the range of 400 to 650 fmol/mg of membrane protein (Table 2), which is within 2-fold of the determined expression levels of endogenous β_2-AR (~300 fmol/mg) in these cells after butyrate treatment (Table 2). We found that both α_{1A}- and β_2-AR expression in these cells could be up-regulated by

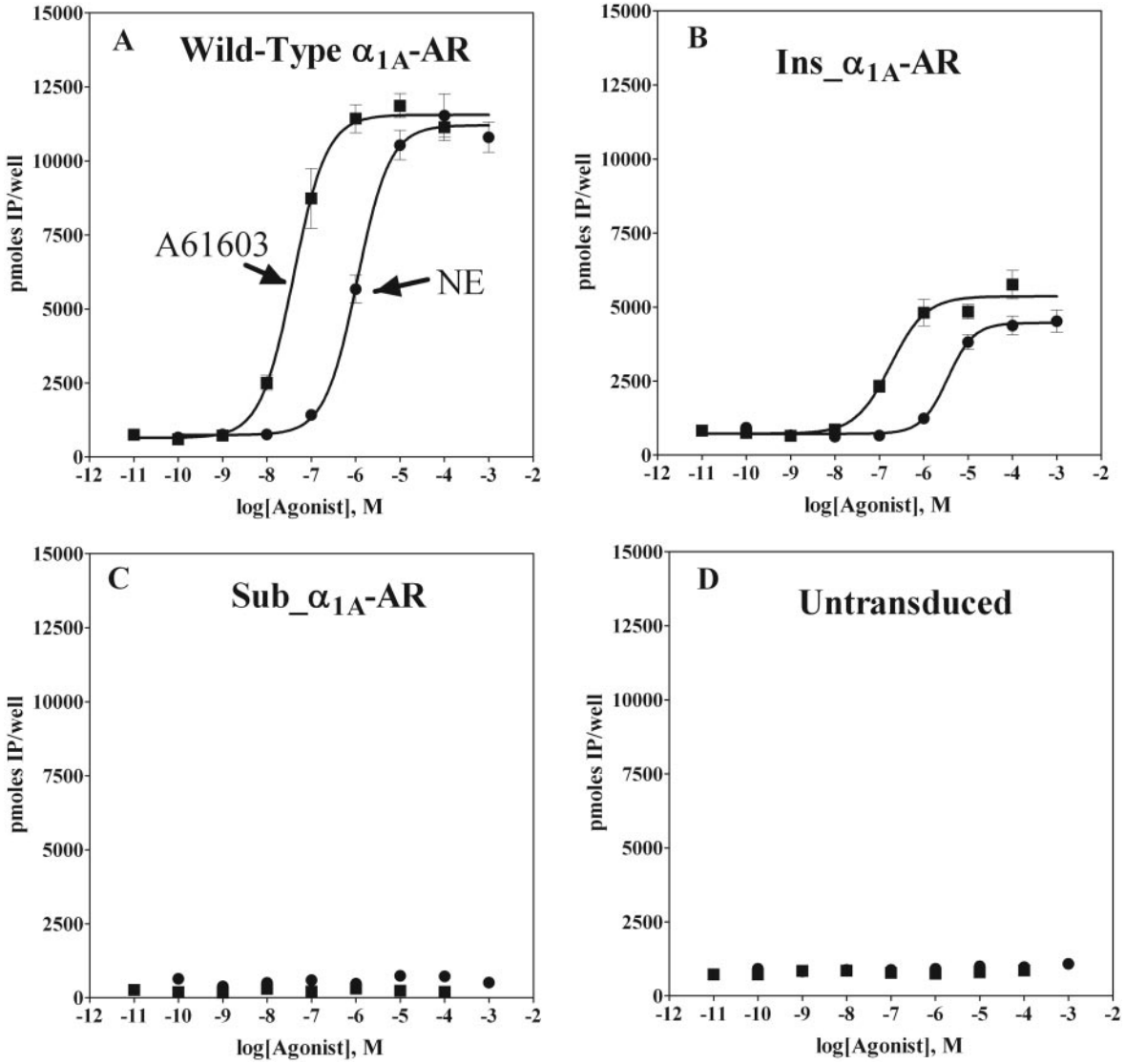

Fig. 1. Inositol phosphate accumulation after stimulation of transduced or untransduced HEK-293/EBNA cells with NE or A61603. HEK-293/EBNA cells transduced with baculovirus strains carrying wild-type (A), Ins_α_{1A}-AR (B), or Sub_α_{1A}-AR (C) along with parental control cells (D) were pretreated with NaBu for 18 h to induce receptor expression. Cells were then plated and NE (●) or A61603 (■) was applied for 20 min, followed by termination of reaction with lysis buffer and quantification of IP. A representative experiment is shown in which each data point is the average value of triplicate samples.

addition of butyrate, a nonselective histone deacetylase inhibitor (Boffa et al., 1978). In naive cells, this treatment seems to enhance signals from endogenous Ca^{2+} channels in response to β_2-AR activation, providing us with a dynamic measure for the induction of cAMP or other mediators by following changes in Ca^{2+} mobilization not observed in untreated, parental HEK-293 cells. Thus, we have a cell-based system to monitor real-time signaling events involving α_{1A} and β_2 adrenoceptor activation, using fluorescence imaging of Ca^{2+} changes as a functional measure.

Incubation of untransduced, NaBu-treated cells with the nonselective adrenoceptor agonist NE induced a transient elevation of cytosolic Ca^{2+} (Fig. 2A). The observed kinetics of the Ca^{2+} rise were relatively slow, with a consistent 10-s delay for the onset of the signal after agonist addition (Fig. 2A, ∗). The maximal Ca^{2+} transient was observed within 40 s from NE addition, for most concentrations tested. This signal quickly decreased and did not trigger the activation of store-operated Ca^{2+} (SOC) channels or any other Ca^{2+} re-entry mechanism, because the Ca^{2+} signal quickly returned to the basal level. We have tested several other β_2-AR-selective and -nonselective agonists, such as fenoterol, procaterol, salbutamol, and isoproterenol. All agonists examined evoked equivalent changes in intracellular Ca^{2+} release, with the expected rank order of potencies (Fig. 3A). In contrast, the β_1-AR selective agonist xamoterol elicited no signals. Consistent with this, the observed agonist signals were sensitive to low concentrations (10 nM) of the β-AR selective antagonists propranolol (data not shown) and ICI 118551 (β_2-selective), but not to the α_1- selective antagonist prazosin (A. Copik, unpublished results) or the β_1-AR antagonist atenolol (Fig. 3B). We did not detect any signals upon treatment of untransduced cells with the α_{1A}-AR selective agonist A61603 (Fig. 2B, ∗), confirming the absence of this receptor in the parental HEK-293 cells. NE-induced Ca^{2+} mobilization in untransduced cells was sensitive to MDL12,330A and H89, the adenylate cyclase and PKA inhibitors, respectively, suggesting that the observed changes in intracellular Ca^{2+} are related to the activation of the G_s pathway (Fig. 3C). Taken together, these results clearly indicate that the slow Ca^{2+} mobilization observed in naive cells is derived from the activation of endogenous β_2-ARs. Consistent with this, the kinetics of the Ca^{2+} transient paralleled the dynamics of cAMP changes induced upon β_2-AR stimulation in these cells, as previously established using the cAMP sensor known as exchange protein directly activated by cAMP and cyclic nucleotide-gated channels as reporters (Violin et al., 2008).

The Ca^{2+} signaling properties of cells transduced with wild-type α_{1A}-AR were clearly differentiated from untransduced controls. Upon addition of NE or the α_{1A}-AR selective agonist A61603, we observed a fast increase in intracellular Ca^{2+} followed by a long-lasting (over several minutes; data not shown) sustained phase (Fig. 2, A and B, ○). The initial fast response is typical of G_q-mediated production of IP_3, which in turn triggers the activation of the endoplasmic reticulum IP_3R and release of Ca^{2+} from that intracellular compartment (Minneman, 1988; for review, see Clapham, 2007). The ensuing sustained phase is presumed attributable to further mobilization of Ca^{2+} from the extracellular compartment, mediated by store-operated Ca^{2+} channels (Bugaj et al., 2005) because it is dependent upon presence of extracellular Ca^{2+} (data not shown). Although responses to both agonists seemed to be the same in their biphasic nature and kinetics of the initial calcium rise, closer inspection indicates noticeable differences in the temporal resolution of the transient phase between A61603- and NE-evoked signals. The transient response to NE seems to have a broader, longer-lasting maximum relative to the one observed with the selective agonist A61603. The ratios of the transient peak response over the sustained phase are also noticeably different

TABLE 1

Pharmacological parameters determined from IP accumulation and Ca^{2+} mobilization assays performed with transiently transduced HEK-293/EBNA cells

Data were fitted to a sigmoidal dose-response equation using the Prism software package to determine EC_{50} and maximal response values.

Agonist	EC_{50}		Intrinsic Activity	
	IP	Ca^{2+}	IP	Ca^{2+}
	μM			
Wild-type α_{1A}-AR				
NE	0.90 ± 0.20	0.070 ± 0.010	1.00[a]	1.00
A61603	0.040 ± 0.020	0.0027 ± 0.0006	1.07	0.86
Ins_α_{1A}-AR				
NE	4.0 ± 2.0	0.13 ± 0.05	1.00	1.00
A61603	0.20 ± 0.10	0.0060 ± 0.0010	1.07	0.56
Sub_α_{1A}-AR				
NE	B.Q.L.	B.Q.L.	B.Q.L.	B.Q.L.
A61603	B.Q.L.	B.Q.L.	B.Q.L.	B.Q.L.
Untransduced				
NE	B.Q.L.	0.50 ± 0.10	B.Q.L.	1.00
A61603	B.Q.L.	B.Q.L.	B.Q.L.	B.Q.L.

B.Q.L., below quantifiable levels.
[a] Relative to NE.

TABLE 2

Binding parameters

B_{max} and K_d values determined from [^{3}H]Prazosin and ^{125}I-CYP saturation binding experiments performed with crude membranes derived from transiently transduced HEK-293/EBNA cells or stably transfected CHO_α_{1A}-AR cells. K_i values were calculated from radioligand competition binding assays carried out with the same membranes. [^{3}H]Prazosin was used as a radioligand in competition assays with membranes derived from cells expressing α_{1A}-AR, whereas ^{125}I-CYP was used with membranes from parental and butyrate-treated HEK-293/EBNA cells.

Construct	[^{3}H]Prazosin		^{125}I-CYP		K_i		
	K_d	B_{max}	K_d	B_{max}	NE	A61603	Oxymet
	nM	*fmol/mg*	*nM*	*fmol/mg*	*mM*	*mM*	*mM*
HEK-293/EBNA	N.B.	N.B.	46	11	34[a]	729[a]	185[a]
HEK-293/EBNA NaBu-treated	N.B.	N.B.	65	274	24[a]	1161[a]	265[a]
HEK-293/EBNA α_{1A}-AR	0.6	410 ± 90	N.D.	N.D.	3.1 ± 1.0	0.13 ± 0.02	0.031 ± 0.009
HEK-293/EBNA Ins_α_{1A}-AR	0.5	450 ± 30	N.D.	N.D.	3.5 ± 1.5	0.10 ± 0.03	0.021 ± 0.004
HEK-293/EBNA Sub_α_{1A}-AR	0.6	650 ± 90	N.D.	N.D.	7.7 ± 2.4	0.17 ± 0.07	0.032 ± 0.013
CHO_α_{1A} AR	0.9	1070 ± 50	N.D.	N.D.	1.5 ± 0.4	0.05 ± 0.01	0.013 ± 0.03

N.B., no detectable binding; N.D., not determined.
[a] ^{125}I-CYP used as a radioligand.

for these two α_{1A}-AR agonists (1.2 for NE and 1.4 for A61603, at maximal response).

Engineered α_{1A}-AR Variants Reveal Signaling Crossover with β_2-ARs. The observed differences in the temporal resolution of the transient phases of Ca^{2+} mobilization between NE and A61603 in wild-type α_{1A}-ARs were even more pronounced in cells expressing the partially active mutant Ins_α_{1A}-AR (Fig. 2, A and B, ■). In these cells, the initial Ca^{2+} rise reached maximum at a later time point for NE-evoked response (24 s) relative to A61603 (13 s), even though the NE peak was somewhat larger in amplitude (2.57 versus 2.14). Stimulation of cells expressing the second variant, Sub_α_{1A}-AR, with NE produced a change in intracellular Ca^{2+} with a temporal resolution corresponding to the stimulation of endogenous β_2-AR yet with significantly increased maximum response amplitude relative to untransduced cells (Fig. 2A, ▲). A61603 produced a very small and extremely slow increase in Ca^{2+} mobilization, manifesting a dramatic signaling deficiency in that modified receptor (Fig. 2B, ▲). Therefore, our findings with these variants confirm that NE stimulation of α_{1A}-AR_HEK-293 cells elicits a Ca^{2+} response comprising more than one phase, involving contributions from canonical α_{1A}- and β_2-AR pathways, and seemingly noncanonical ones originating from these same receptors, yet to be resolved.

To examine the potency and response magnitude of the

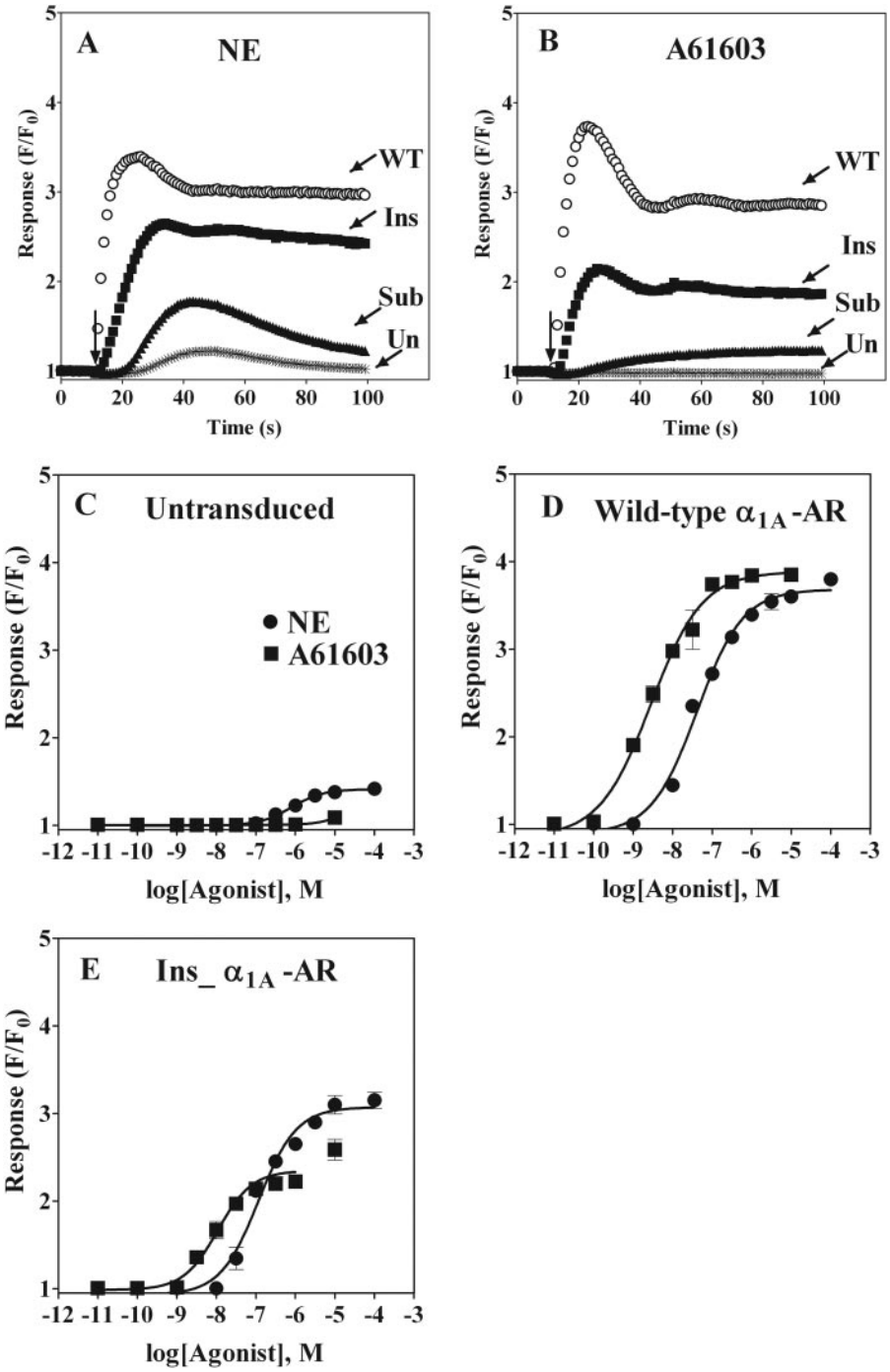

Fig. 2. Ca^{2+} mobilization in transduced HEK-293/EBNA cells upon stimulation with norepinephrine (NE) or A61603. Cells were transduced with baculoviral strains carrying control, wild-type α_{1A}-AR, and ICL3 variants Ins_α_{1A}-AR or Sub_α_{1A}-AR, followed by treatments with NaBu for 18 h before experiments. Cells were then dispensed into 96-well plates and loaded with fluorescent dye. Ca^{2+} transients in response to stimulation with NE or A61603 were monitored fluorometrically. A and B, normalized, time-dependent changes after treatment with 1 μM NE and 100 nM A61603, respectively. Untransduced control (*), wild-type α_{1A}-AR (○), and ICL3 variants Ins_α_{1A}-AR (■) and Sub_α_{1A}-AR (▲). Arrow at 10 s indicates time of agonist addition. C to E, concentration-effect curves for NE-mediated (●) or A61603-mediated (■) Ca^{2+} transient responses in untransduced cells (C) or cells transduced with wild-type (D) and Ins_α_{1A}-AR (E). Data points represent peak fluorescence values of the recorded Ca^{2+} transients in response to agonist addition and are reported relative to baseline values measured 10 s before addition. Each experiment was performed three independent times, with duplicates.

adrenoceptor agonists NE and A61603 in untransduced cells (Fig. 2C) and cells transiently transduced with wild-type α_{1A}-AR (Fig. 2D) or the Ins_α_{1A}-AR (Fig. 2E), we quantified the fast onset response peak amplitude (F/F_0) of Ca^{2+} responses as a function of agonist concentration. The selective α_{1A}-AR agonist A61603 produced dose-dependent Ca^{2+} responses only in α_{1A}-AR transduced cells. The EC_{50} values were 3 nM for wild-type α_{1A}-AR and 6 nM for Ins_α_{1A}-AR

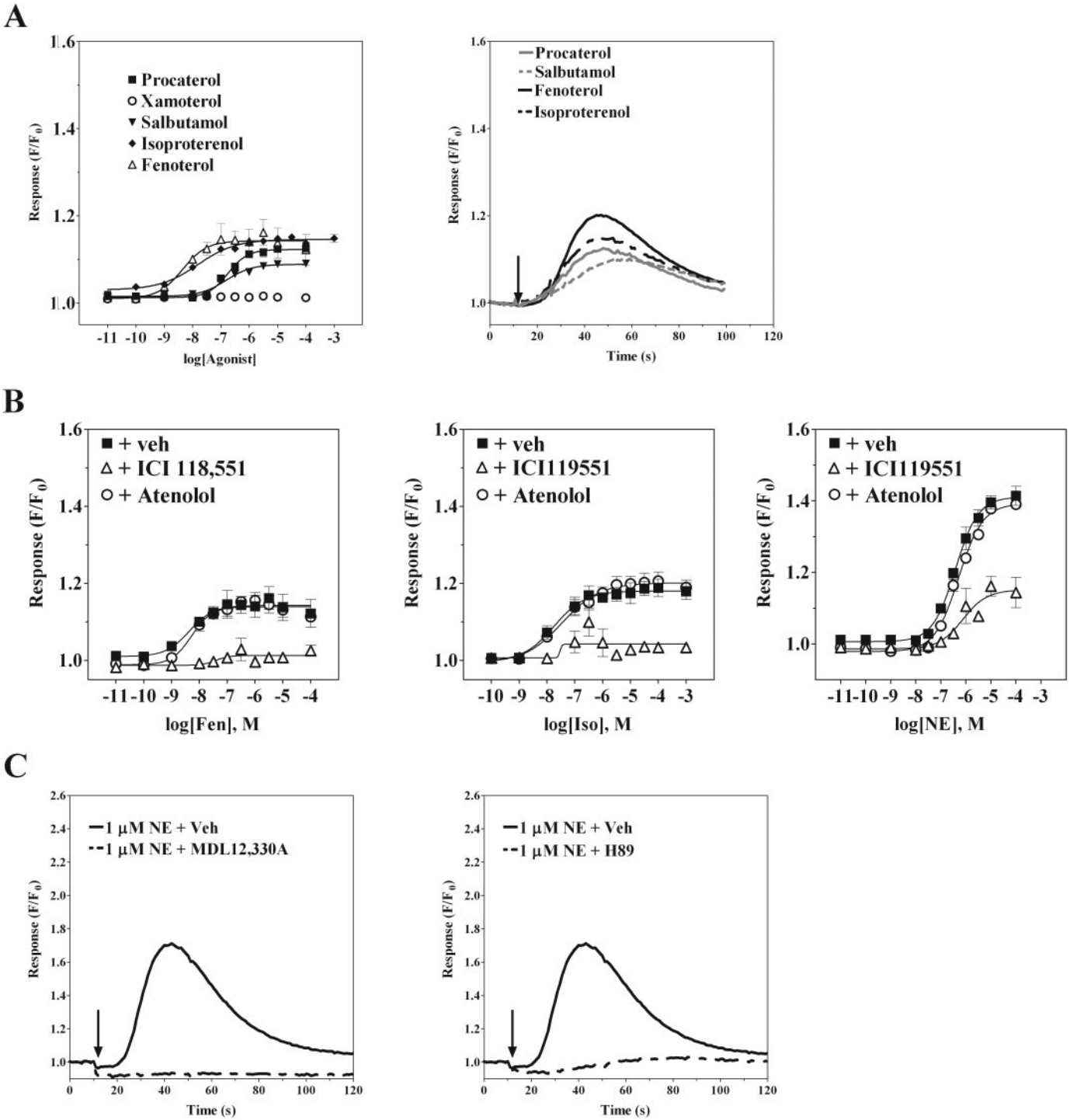

Fig. 3. Ca^{2+} mobilization in untransduced, NaBu-treated HEK-293/EBNA cells upon stimulation with β-AR agonist. HEK-293/EBNA cells were treated with NaBu for 18 h before experiments. Cells were then plated on 96-well plates, loaded with fluorescent dye (*Materials and Methods*) and washed. A, left, cells were treated with increasing concentrations of procaterol (■), xamoterol (○), salbutamol (▼), fenoterol (△), or isoproterenol (◆). Right, kinetics of Ca^{2+} mobilization in the same cells treated with 3 μM procaterol (solid gray line), salbutamol (dashed gray line), fenoterol (solid black line), or isoproterenol (dashed black line). B, a second set of cells was pretreated with vehicle (■), 10 nM ICI118551 (△), or 1 μM atenolol (○) for 5 min and stimulated with increasing doses of NE (right), isoproterenol (center) or fenoterol (left). C, cells were pretreated with vehicle (solid black line), 25 μM MDL12,330A (left, dashed black line) or H89 (right, dashed black line) for 30 min and stimulated with 1 μM NE. Changes in cytoplasmic Ca^{2+} levels were monitored by fluorometry. Data points represent peak fluorescence values of the recorded Ca^{2+} transients in response to agonist addition and are reported relative to baseline values measured 10 s before addition. Each experiment was performed two independent times, with duplicates.

(Table 1). This early peak was absent from the Sub_α_{1A}-AR calcium responses precluding determination of dose dependence correlation. As mentioned above, for the nonselective adrenoceptor agonist NE, the time course for Ca^{2+} transient responses is complex, making it difficult to isolate the effect of this ligand resulting solely from activation of α_{1A}-AR cells. For this agonist, peak responses occurred at 13 and 26 s from agonist addition, for wild-type α_{1A}-AR cells (apparent EC_{50} value of 70 nM) and Ins_α_{1A}-AR cells (EC_{50} = 130 nM), respectively (Table 1). It is remarkable that even though NE and A61603 are both full agonists, A61603 showed only partial agonism relative to NE at the Ins_α_{1A}-AR variant, the only one amenable to quantification (Table 1). This differential signaling efficacy may account for the observed slowdown of the initial NE calcium peak, resulting in an overall transient that is shifted toward the maximum observed for the β_2-AR Ca^{2+} response. At a first approximation, this suggests a level of synergy in cross-talk between α_{1A}- and β_2-adrenoceptors in this system, because only NE will activate both subtypes. However, the activation of β_2-AR does not seem to change the response properties of α_{1A}-AR at G_q, because both the selective and the nonselective agonists induced similar levels of IP accumulation (Fig. 1), a more proximal measure for G_q coupling. Therefore, the observed higher efficacy of NE, compared with A61603, to induce Ca^{2+}-mobilization in cells expressing Ins_α_{1A}-AR seems to reveal a component contributed by activation of endogenous β_2-ARs.

To resolve the contribution of the β_2-AR initiated signaling to the measured calcium mobilization, we studied the kinetics of response to NE and A61603 in the presence and absence of the β-selective antagonist propranolol at a saturating concentration (100 nM). Inhibition of the β_2-AR with propanolol eliminated the observed differences in the kinetics of NE versus A61603-induced Ca^{2+} mobilization in wild-type α_{1A}-AR-transduced cells (Fig. 4, A and B). Thus, β-AR blockade made the NE Ca^{2+} response profile look similar to the one observed with A61603: a fast and transient peak of intracellular calcium followed by a long-lasting, sustained phase. The ratio between the Ca^{2+} changes observed in the transient phase over the sustained phase (~1.4), and the kinetics of the initial Ca^{2+} rise were similar for both agonists in the presence of propanolol. The pharmacological behavior of the insertion ICL-3 variant was consistent with the following: the activation kinetics of cells expressing the partially active mutant Ins_α_{1A}-AR with either agonist in the presence of 100 nM propranolol was virtually identical to the one observed with wild-type α_{1A}-AR cells, with smaller amplitudes for both the early calcium peak and the sustained phase (Fig. 4, C and D). Responses of the Sub_α_{1A}-AR variant were almost entirely eliminated by addition of 100 nM propranolol. Only a minimal and extremely slow (over 100 s)

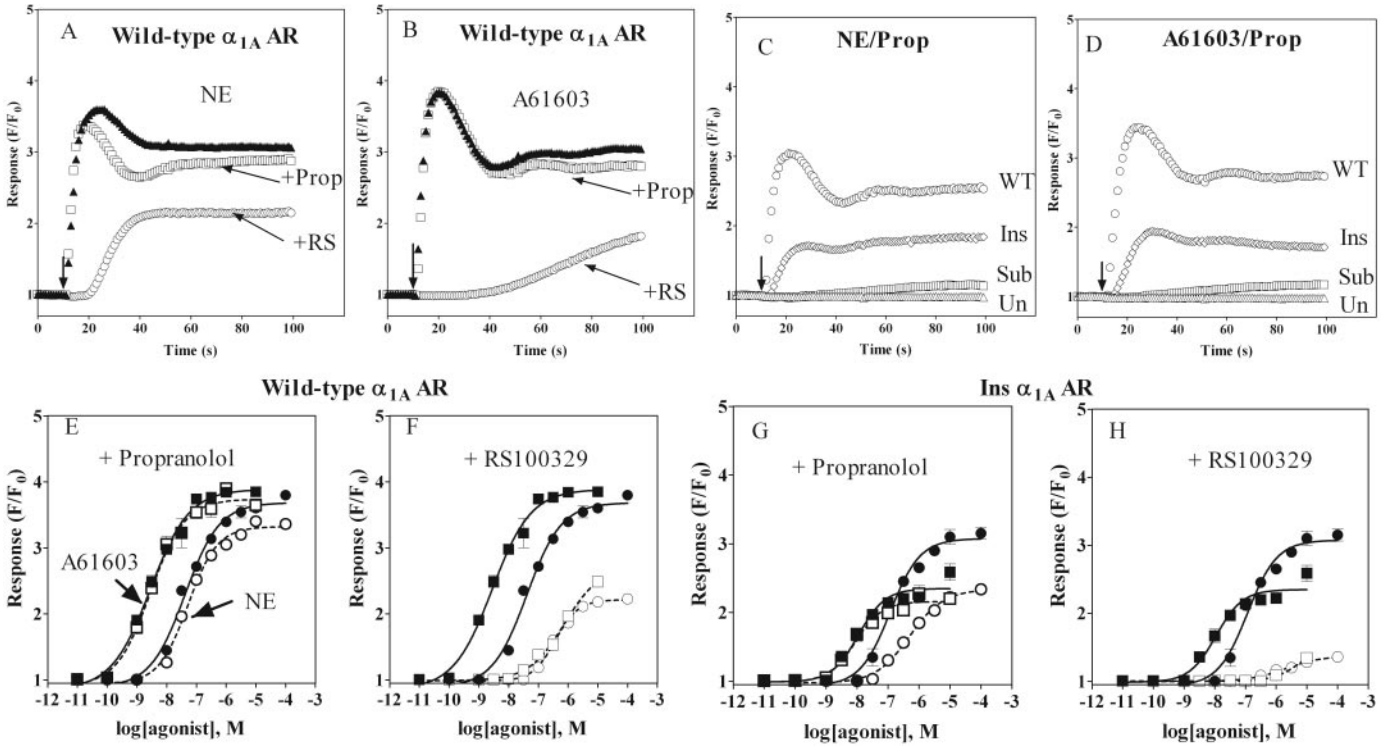

Fig. 4. Ca^{2+} mobilization in transduced HEK-293/EBNA cells upon stimulation with NE or A61603 in presence of α_{1A}- and β-AR selective antagonists. Cells were transduced with baculovirus stocks encoding wild-type or the ICL3 α_{1A}-AR variants, followed by 18-h treatment with NaBu and measurement of Ca^{2+} transient response. A and B, fluorescence changes relative to baseline (F/F_0) in wild-type α_{1A}-AR_HEK-293/EBNA cells pretreated for 10 min with vehicle (▲), 100 nM propranolol (□), or 100 nM RS100329 (○) followed by stimulation with 1 μM NE (A) or 100 nM A61603 (B). Arrows indicate the time of agonist addition. C and D, kinetics of NE-induced (C) or A61603-induced (D) Ca^{2+} mobilization observed in HEK-293/EBNA cells transduced with control (△), wild-type (○), Ins_α_{1A}-AR (◇), or Sub_α_{1A}-AR (□) baculoviral strains after propranolol (Prop) pretreatment (10 nM, 10 min). Cells expressing wild-type α_{1A}-AR (E and F) or Ins_α_{1A}-AR (G and H) were pretreated with either 100 nM propranolol (E and G, open symbols) or 100 nM RS100329 (F and H, open symbols), followed by incubation for 5 min. Each plate also contained control wells with cells that were pretreated with vehicle under the same conditions (E to H, filled symbols). Concentration-effect curves of A61603 (■, □) or NE (●, ○)-mediated Ca^{2+} transient responses were determined from peak fluorescence relative to baseline (F/F_0), plotted against agonist concentration. Data points are representative of three independent measurements with duplicate (controls) or triplicate (agonist-treated) samples. Data points reflect the average values of duplicate samples.

increase in Ca^{2+} was detected, confirming our initial interpretation that this ICL-3 modification renders that α_{1A}-AR variant incompetent for direct signaling (Fig. 4, C and D). No responses could be detected in control untransduced cells pretreated with 100 nM propranolol (Fig. 4, C and D).

Effects of Agonist Occupancy at β_2-ARs on the Pharmacological Behavior of α_{1A}-ARs. In wild-type α_{1A}-AR cells, responses are primarily driven by the fast G_q-mediated release of Ca^{2+} from the endoplasmic reticulum. Therefore, the concentration-response to NE or A61603 that was derived from the magnitude of the initial phase of intracellular Ca^{2+} mobilization should not be affected by ligands acting at β_2-ARs. Indeed, we found that preincubation with propranolol had no significant effect on the dose-response curves of NE or A61603 (Fig. 4E). However, in cells expressing variant α_{1A} adrenoceptors, the NE dose-response curve in the presence and absence of 100 nM propranolol revealed that this β-selective antagonist significantly decreased NE responses, with only a modest effect on the EC_{50} value (Fig. 4G). In fact, for Ins_α_{1A}-AR transduced cells, the maximal response of NE in the presence of propranolol was equal to that of A61603, consistent with the contribution of β_2-AR to observed signals (Fig. 4G). The lack of an effect of propranolol on the EC_{50} values of these agonists at α_{1A}-AR transduced cells suggests that this β-selective AR antagonist either acts solely by blocking β-AR signaling or, alternatively, as a noncompetitive antagonist at α_{1A}-AR sites. We interpret these results as an indication that β_2-ARs require agonist occupancy and activation to exert an effect on α_{1A}-AR initiated signaling. In addition, the presence of antagonist-bound β_2-AR has no bearing on α_{1A}-AR Ca^{2+} signaling. Thus, we saw no evidence in this system for inverse agonism or β-adrenoceptor constitutive activity.

We also studied the effect of pretreating transduced cells with the α_{1A}-AR selective antagonist RS100329 (Williams et al., 1999) at a saturating concentration (100 nM). We observed rightward shifts for the EC_{50} values of both A61603 (3–800 nM at wild-type and 10–400 nM at Ins_α_{1A} AR) and NE (0.07–0.6 μM at wild-type and 0.1–2 μM at Ins_α_{1A}-AR; Fig. 4, F and H, closed versus open symbols). It is noteworthy that this EC_{50} shift in the presence of RS100329 was more than one log greater for A61603 relative to NE, indicating that part of the response to NE alone is mediated via additional receptors to α_{1A}-AR. The remaining activity that we observed with NE after treatment with RS100329 could be attributed to its action at β_2-ARs, unlikely to be antagonized by RS100329 at 100 nM (Fig. 4, F and H). The antagonistic effect of RS100329 seemed to be partially insurmountable, probably because of incomplete achievement of equilibrium conditions (hemi-equilibrium condition) over the course of our Ca^{2+} recordings (Kenakin, 2004). Such pseudo-irreversible antagonism stems from the relatively slow rates of dissociation for antagonist relative to the short acquisition time of the experiment (Kenakin, 2004). This is also indicated by the Ca^{2+} mobilization profiles of wild-type α_{1A}-AR cells pretreated with RS100329, followed by stimulation with A61603: a slow, linear increase in Ca^{2+} was observed under those conditions (Fig. 4B). After treatment of those cells with RS100329, application of NE elicited a response with a 10-s delay in the Ca^{2+} rise (Fig. 4A). The signals lacked any observable desensitization or rapid return to baseline. This may be due to slow recovery of α_{1A}-AR signaling upon dissociation of RS100329 from the receptor, inherent to the nonequilibrium nature of transient measurements.

To further address whether activated β_2-ARs influence the signaling behavior of coexpressed α_{1A}-ARs, we performed concentration-response analysis of A61603 and NE-mediated signaling in the presence or absence of a fixed concentration of the potent β-AR agonist isoproterenol (at $EC_{75} \sim 10$ nM). NE is a fairly low-affinity agonist at both β_2- and α_{1A}-ARs (Perez, 2005), thus the level of both α_{1A}- and β_2-AR activation should change with increasing concentrations of NE in α_{1A}-AR transduced EBNA cells. We simplified our experimental system by keeping the occupancy (and activation) of β_2-ARs constant, by concomitant application of α_{1A}-AR agonists and isoproterenol, assuming there is no influence of agonist occupancy at α_{1A}-AR on that of the β_2-AR. As expected for untransduced cells, there were no responses to A61603 and only background responses to isoproterenol and NE were observed (Fig. 5, A and E). Simultaneous stimulation of wild-type α_{1A}-AR cells with increasing concentrations of NE plus 10 nM isoproterenol resulted in dose-dependent increases in intracellular Ca^{2+} (Fig. 5B). The EC_{50} was shifted to the left by roughly 1 log unit (EC_{50} = 0.008 μM) relative to measurements in the absence of isoproterenol (EC_{50} = 0.06 μM), indicating that this β-selective agonist acted as a potentiator of the α_{1A}-AR response. The same effect was observed with A61603, although isoproterenol also increased the apparent maximum response to A61603 by approximately 20% (F/F_0 = 3.1 and 3.5 at maximally effective A61603). The observed increase in A61603 maximal effect in the presence of 10 nM isoproterenol became more evident in experiments employing cells expressing the α_{1A}-AR ICL-3 variants (Fig. 5, C and D). Because both mutants displayed a Ca^{2+} phase consistent with β_2-driven response (slow-rising peak with a maximum at 37 s after agonist addition), quantification of agonist potency and response amplitude was possible for Sub_α_{1A}-AR (Fig. 5, G and H). Isoproterenol (10 nM) increased A61603 responses by 160% (F/F_0 = 1.8 and 3.1) and 500% (F/F_0 = 1.1 and 1.9) for the Ins_α_{1A}-AR and Sub_α_{1A}-AR cells, respectively (Fig. 5, C and D). In all cases, the kinetics and amplitude of combined A61603 plus isoproterenol roughly equaled the response kinetics and amplitude of NE by itself (Fig. 5, F–H).

More importantly, in the presence of 10 nM isoproterenol, A61603 induced a dose-dependent Ca^{2+} mobilization in cells expressing the coupling-deficient Sub_α_{1A}-AR variant (Fig. 5D). The observed EC_{50} value of 5 nM was comparable with the EC_{50} of A61603 alone at wild-type_α_{1A}-AR cells, and 1 log less potent than that observed for A61603 at wild-type α_{1A}-ARs in the presence of isoproterenol. This value is at least 1000-fold more potent relative to the EC_{50} of A61603 at β_2-ARs. This suggests that the observed response occurs upon A61603 occupancy of Sub_α_{1A}-ARs only when β_2-ARs are simultaneously agonist activated. The necessity for β_2-AR activation is also evidenced by the time course of the induced Ca^{2+} rise, which clearly displays β_2-AR features: 10-s delay for the rise and return to baseline within the recording time window, consistent with receptor desensitization (Fig. 5H). Thus, the isoproterenol-induced potentiation of the A61603-evoked calcium mobilization in Sub_α_{1A}-AR cells indicates that this variant, virtually devoid of signaling activity (no Ca^{2+} or IP response to A61603), was still able to interact with β_2-AR. As mentioned above, A61603 did not

effect dose-dependent Ca^{2+} mobilization in untransduced cells, even in the presence of isoproterenol (Fig. 5A). Therefore, this observation confirms that the response of Sub_α_{1A}-AR cells cannot be a consequence of direct action of A61603 at β_2-AR.

One way of rationalizing our results is to postulate the formation of α_{1A}/β_2-AR heterodimers, in which activation of the β_2-AR counterpart "rescues" the signaling capacity of the defective α_{1A}-AR variant. It has been proposed that both GPCR homo- and heterodimers can transactivate in a cooperative fashion to couple to associated G proteins (Carrillo et al., 2003). The ability of the selective α_{1A} agonist A61603 to increase isoproterenol-mediated β_2-AR responses in cells expressing the signaling-defective mutant Sub_α_{1A}-AR is consistent with the concept of cooperative transactivation, in which A61603-induced conformational changes in α_{1A}-AR mediate the transactivation of the associated functional β_2-AR and its signaling. This is not surprising, because the position of the CCPGCC substitution in the ICL3 of this variant is likely to interfere with G protein-receptor interaction but not with ligand binding or conformational transitions resulting from that event (for review, see Oldham and Hamm, 2007; Perez, 2007). As a corollary, the β-AR selective agonist isoproterenol induced downstream signaling from Sub_α_{1A}-AR, reflecting a non-G_q coupling mode (see *Pharmacological Dissection of α_{1A}-AR Signaling Events*). Therefore, this cooperative effect occurred in both directions.

Contributions of cAMP-Mediated Signaling to the α_{1A}/β_2-AR Cross-Talk. An alternate interpretation to the heterodimer hypothesis involves crossover of signals downstream from α_{1A}- and β_2-ARs. To address this possibility, we used two different approaches. First, we asked whether the observed cross-talk was specific to β_2-AR signaling. For this, we examined the effects of forskolin, a direct activator of adenylyl cyclase that bypasses β_2-AR, and of NECA, an agonist of the G_s-coupled adenosine 2B receptor, endogenously expressed in HEK-293 cells (Cooper et al., 1997). Stimulation with 50 μM forskolin or NECA in the absence of the α_{1A}-AR agonist A61603 resulted in Ca^{2+} mobilization with similar temporal resolution to each other in both naive and α_{1A}-AR transduced cells (Fig. 6, A and C). This validates the assumption that our experiments report on Ca^{2+} mobilization related to increases in intracellular cAMP. However, responses were much slower than the ones observed with β_2-AR agonists, reaching maximal levels only over 70 s from the time of compound addition. Those transients were also more persistent, suggesting a signaling mechanism less prone to desensitization. As expected, stimulation of naive cells with increasing concentrations of A61603 in the absence or presence of 50 μM forskolin or NECA did not result in a concentration-dependent mobilization of calcium (Fig. 6B). Stimulation of α_{1A}-AR-transduced cells with A61603 resulted in dose-dependent increases in intracellular calcium (EC_{50} = 3.1 nM) that were unaffected by costimulation with forskolin (EC_{50} = 1.4 nM) and only marginally potentiated by costimulation with NECA (EC_{50} = 0.9 nM; Fig. 6D). Only NECA increased the response magnitude to A61603 modestly, by approximately 10%. Therefore, neither forskolin nor NECA recapitulated the calcium mobilization effects observed upon costimulation of cells with A61603 and isoproterenol.

Close examination of Ca^{2+} signal's time course indicates that both NECA and forskolin affected minimally the fast,

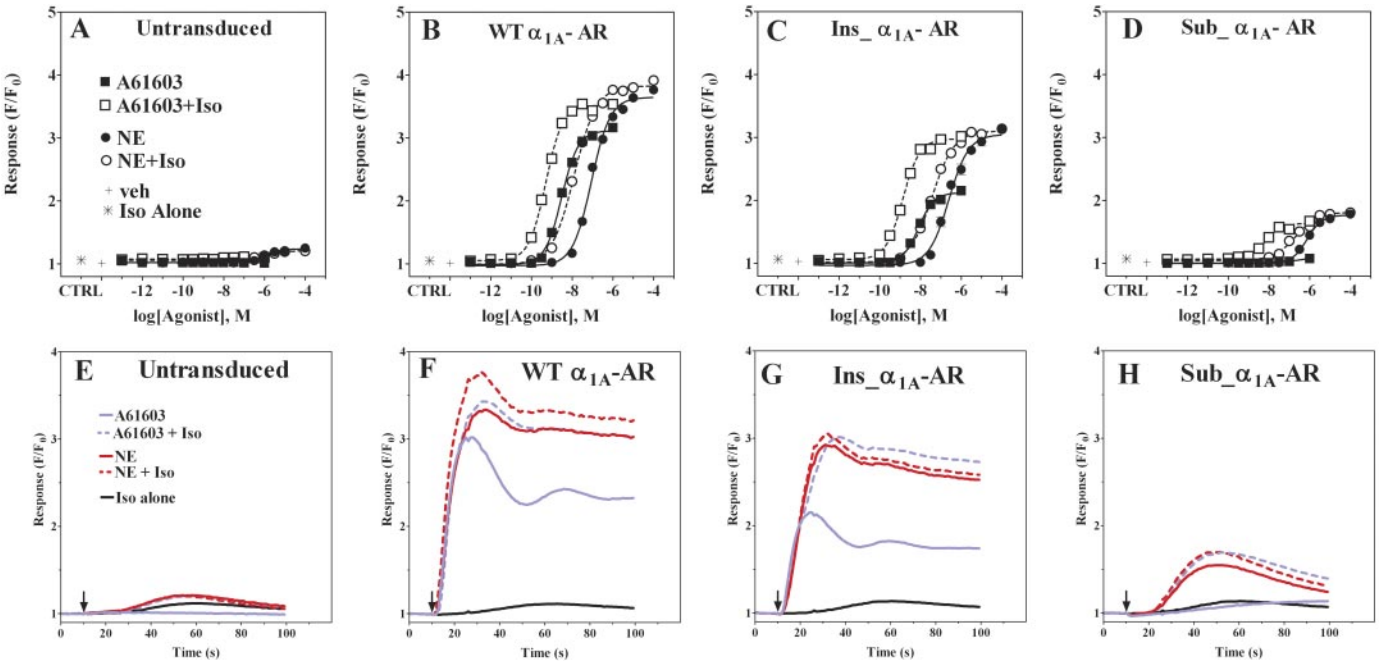

Fig. 5. Potentiation of the agonist-evoked rise in cytoplasmic Ca^{2+} by 10 nM isoproterenol. HEK-293/EBNA cells were transduced with control (A and E), wild-type (B and F), Ins_α_{1A}-AR (C and G), or Sub_α_{1A}-AR (D and H) baculoviral strains, followed by 18-h treatment with NaBu and measurement of Ca^{2+} transient response. A to D: concentration-effect relationship of responses to simultaneous application of 10 nM isoproterenol (open symbols) or vehicle (filled symbols) and increasing concentrations of A61603 (■, □) or NE (●, ○). Normalized fluorescence changes were recorded versus time. Dose-response data show peak fluorescence values over baseline. Plots represent one of four independent experiments, data points reflect the average values of duplicate samples. E to H, kinetics of Ca^{2+} mobilization observed in HEK-293/EBNA cells transduced with control (E), wild-type α_{1A}-AR (F), Ins_α_{1A}-AR (G), or Sub_α_{1A}-AR (H) baculoviruses exposed to 100 nM A61603 (blue) or 1 μM NE (red), in the presence (dashed line) or absence (solid line) of 10 nM isoproterenol. The black solid line depicts the response to stimulation with 10 nM isoproterenol alone. Arrows indicate the time of agonist addition. Plots represent one of four independent experiments, data points reflect the average values of duplicate samples.

transient phase (Fig. 6C). Focusing on the sustained phase, forskolin seemed to elevate it with an apparent Ca^{2+} mobilization maximum at 50 s after compound addition. We were surprised that although NECA had the same effect on the sustained phase, it also stimulated an additional component with intermediate kinetics relative to the fast and sustained phases (Fig. 6C). Thus, even though NECA and forskolin contributed to A61603-induced signals from α_{1A}-AR, the mechanism by which they mediate that effect seems to be different: there is no generic effector mechanism induced in these cells upon treatment with NaBu accounting for the β_2-AR effects observed on α_{1A}-AR responses upon costimulation with A61603 and isoproterenol. Consistent with this interpretation, neither NECA nor forskolin recovered dose-

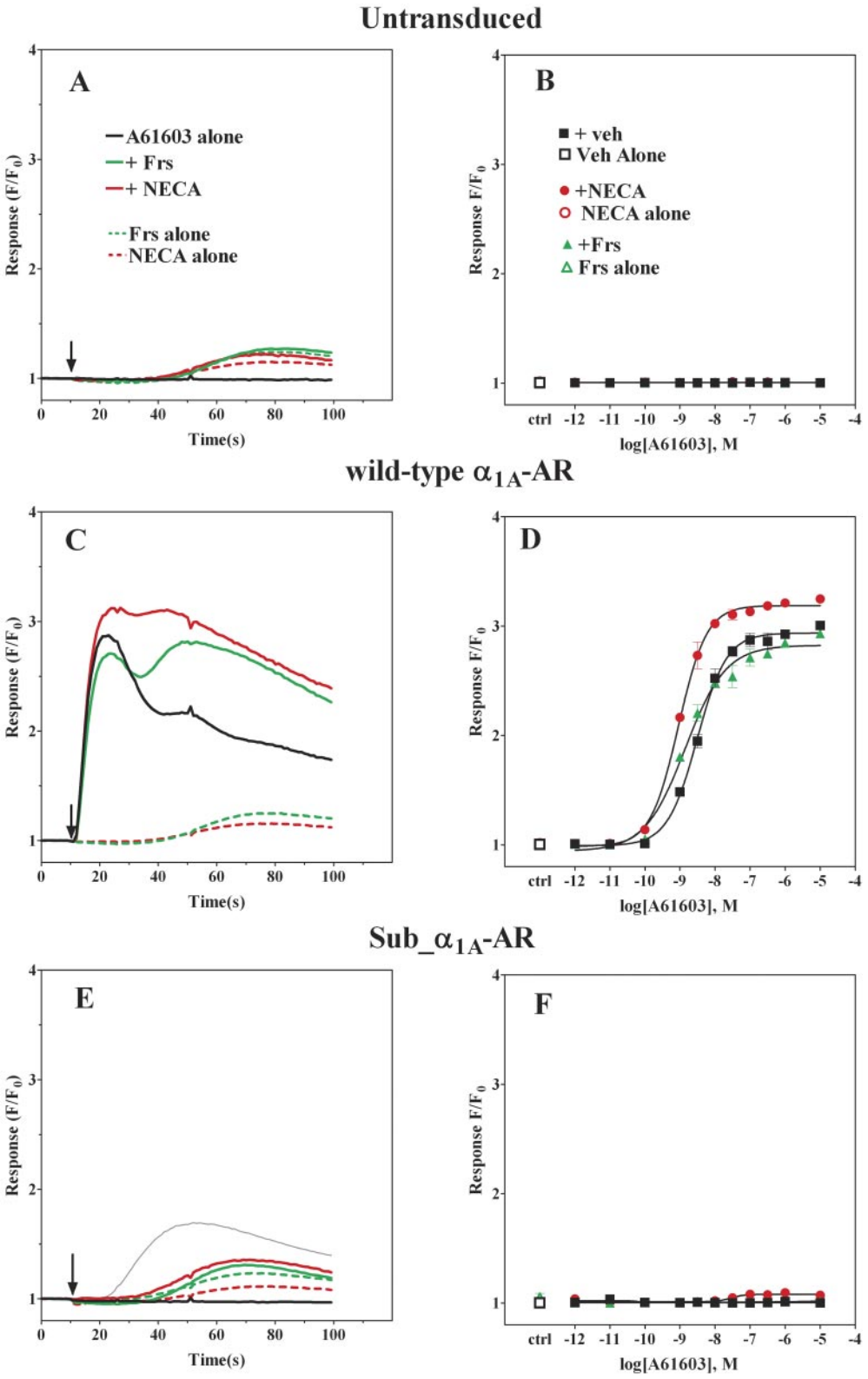

Fig. 6. Potentiation of Ca^{2+} mobilization by 50 μM forskolin (Frs) or 50 μM NECA in HEK-293/EBNA cells. Cells were transduced with control (A and B), wild-type α_{1A}-AR (C and D), or Sub_α_{1A}-AR (E and F) baculoviral stocks. They were then stimulated with increasing concentrations of A61603 in the presence of vehicle (black squares), 50 μM forskolin (green triangles), or 50 μM NECA (red circles) (B, D, and F). Open symbols, effect of forskolin or NECA in absence of A61603. A, C, and E, kinetic traces of calcium mobilization in response to forskolin (green) or NECA (red), in the presence (solid line) or absence (dashed line) of 100 nM A61603. The black solid line depicts response to stimulation by 100 nM A61603 alone, and the gray solid line in E corresponds to Ca^{2+} mobilization in response to stimulation with a combination of 100 nM A61603 and 10 nM isoproterenol in Sub_α_{1A}-AR transduced cells. The agonist was added at the 10-s time point, as indicated by the arrows.

dependent transient responses to A61603 in the Sub_α_{1A} AR variant (Fig. 6F). The dramatic functional rescue of Sub_α_{1A}-AR upon β_2-AR costimulation was just not observed (Fig. 5, D and H). As expected, the kinetics of those effects did not indicate recovery of G_q coupling (Fig. 6E). As a corollary, the absence of functional rescue observed for this variant with either forskolin or NECA in the presence of NaBu further indicates that the pharmacological signatures that we observed are unequivocally dependent on β_2-AR signaling (compare Fig. 6, E and F, with Fig. 5, D and H). Therefore, although these experiments indicate that certain aspects of the cross-talk, such as potentiation of the sustained phase, are directly correlated to generation of cAMP, they do not rule out and actually support the presence of functional α_{1A}/β_2-AR heterodimers.

Pharmacological Dissection of α_{1A}-AR Signaling Events. So far, our studies suggest the presence of an α_{1A}-AR driven, non-G_q signaling pathway that is potentiated by coactivation of β_2-AR. To isolate this component in our Ca^{2+} mobilization measure, we used a combination of xestospongin C and 2-APB, which are inhibitors of IP_3R and SOC channels, respectively. Therefore, this combination should remove from the Ca^{2+} transients any component of the signaling cascade initiated from G_q coupling. As suggested from previous results (Figs. 5F and 6C), wild-type α_{1A}-AR cells stimulated with NE or A61603 after pretreatment with a combination of 5 μM xestospongin C and 20 μM 2-APB exhibited a single phase of Ca^{2+} mobilization, devoid of both the rapid and sustained phases associated with G_q signaling (Fig. 7, red and blue traces). Inclusion of 10 nM isoproterenol in addition to A61603 enhanced this "intermediate" response (Fig. 7, dashed versus solid blue lines). This phase had a maximum at 23 s after agonist addition, approximately 10 s slower than the initial G_q-mediated response. (Fig. 7, black dashed line). It became partly masked by the G_q-induced components observed in α_{1A}-AR cells simultaneously stimulated with A61603 and isoproterenol in the absence of xestospongin C and 2-APB (Fig. 7, black dashed line). These results indicate that additional, noncanonical signaling pathways contribute to intracellular Ca^{2+} mobilization. Thus, the observed intermediate component seems to be strongly tied to β_2-AR activation and apparently unrelated to G_q activation.

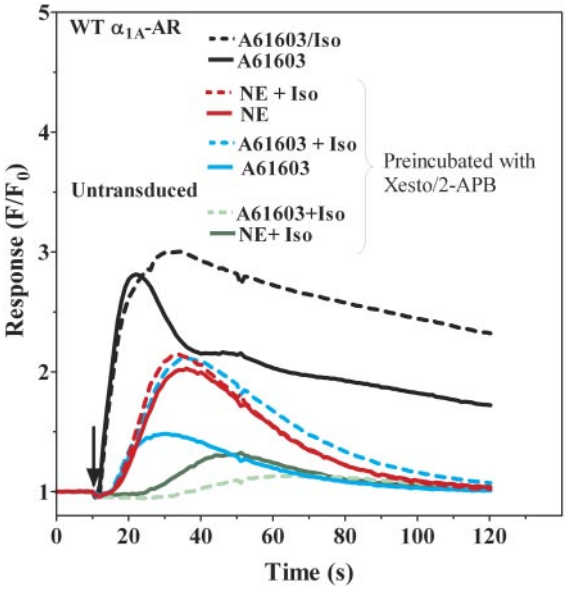

Fig. 7. Effect of IP_3R and Ca^{2+} release activated channels inhibitors on Ca^{2+} mobilization in response to A61603, in the presence or absence of 10 nM isoproterenol. HEK-293/EBNA cells transduced with a wild-type α_{1A}-AR baculoviral stock were pretreated for 30 min with vehicle (black traces), or a combination of 5 μM xestospongin C (Xesto) and 10 μM 2-APB (red and blue traces). Cells were then stimulated with 100 μM A61603 (blue and black traces) or 1 mM NE (red traces) in the presence (broken line) or absence (solid line) of 10 nM isoproterenol. Green traces represent control experiments employing untransduced cells pretreated with xestospongin C and 2-APB (light green broken line, 100 μM A61603 + 10 nM isoproterenol; dark green solid line, 1 mM NE + 10 nM isoproterenol).

Discussion

In summary, here we present a broad range of internally consistent evidence for the functional interaction of α_{1A}- and β_2-adrenoceptors. This provides a conceptual framework for previous preclinical and clinical findings suggesting such interactions. Furthermore, by using a well characterized cell-based model system allowing for manipulation of the expression levels of α_{1A}- and β_2-ARs to mimic physiologically low expression levels, we were able to dissect the signaling components contributing to Ca^{2+} mobilization in response to activation of these two receptors. Relative to most transfection-based gene delivery methods, receptor expression driven by baculoviral gene transduction yields more homogeneous expression levels. This is indicated in FACS plots by the near-Gaussian distribution showing positive kurtosis (leptokurtic distribution) of α_{1A}-AR transduced cells, in which where nearly 80% of them distribute within 3-fold from the geometric mean of the entire population (Supplemental Fig. S1A). At the same time, Supplemental Figure S1, A and B, reveal small populations that display surface levels of α_{1A}-AR expression above or below the bulk of the cells, which may introduce biases either to β_2- or α_{1A}-predominant functional measures. Such small populations of untransduced cells expressing solely β_2-AR as well as α_{1A}-AR-overexpressing cells will always be present, yet they will probably lead to merely additive effects in measured Ca^{2+} mobilization, inconsistent with observations of nonadditivity that we report here.

Figure 8 depicts in a diagrammatic, qualitative fashion the individual components that contribute to the α_{1A}- and β_2-AR-induced transients observed. The first, rapid transient phase peaking at ~12 s after agonist addition reflects the activation of IP_3Rs and Ca^{2+} transfer from the endoplasmic reticulum to the cytoplasm (Fig. 8A). The slower sustained phase depicted in Fig. 8B represents entry of Ca^{2+} from the extracellular compartment after activation of CRAC or other reentry channels. The previously unidentified phase showing intermediate kinetics of Ca^{2+} mobilization (peaking at ~23 s after agonist addition) is revealed only after inhibition of the contributions of IP_3Rs and calcium reentry channels. This component is likely to be mediated by cAMP through a G_q-dependent or -independent mechanism (Fig. 8C), although the precise identity of additional signaling components downstream from β_2-AR and the channel involved in this Ca^{2+} mobilization phase has yet to be identified. The β_2-AR signaling component is shown in Fig. 8D as a delayed response peaking around 30 s, with appreciable desensitization. Finally, the interplay of these phases is illustrated for cells transduced with wild-type α_{1A}-AR (Fig. 8E) or the partially

signaling-defective variant Ins_α_{1A}-AR (Fig. 8F) on costimulation with the endogenously expressed β_2-AR. These last two diagrams show how that potentiation of the intermediate phase by β_2-AR activation becomes apparent only with the partially active mutant, because of the decrease in the rapid transient and slow sustained phases. Although we attempted to build explicit models to account quantitatively for these phases, the inherent nonadditivity of the effects observed upon receptor costimulation precluded construction of an adequate formal model.

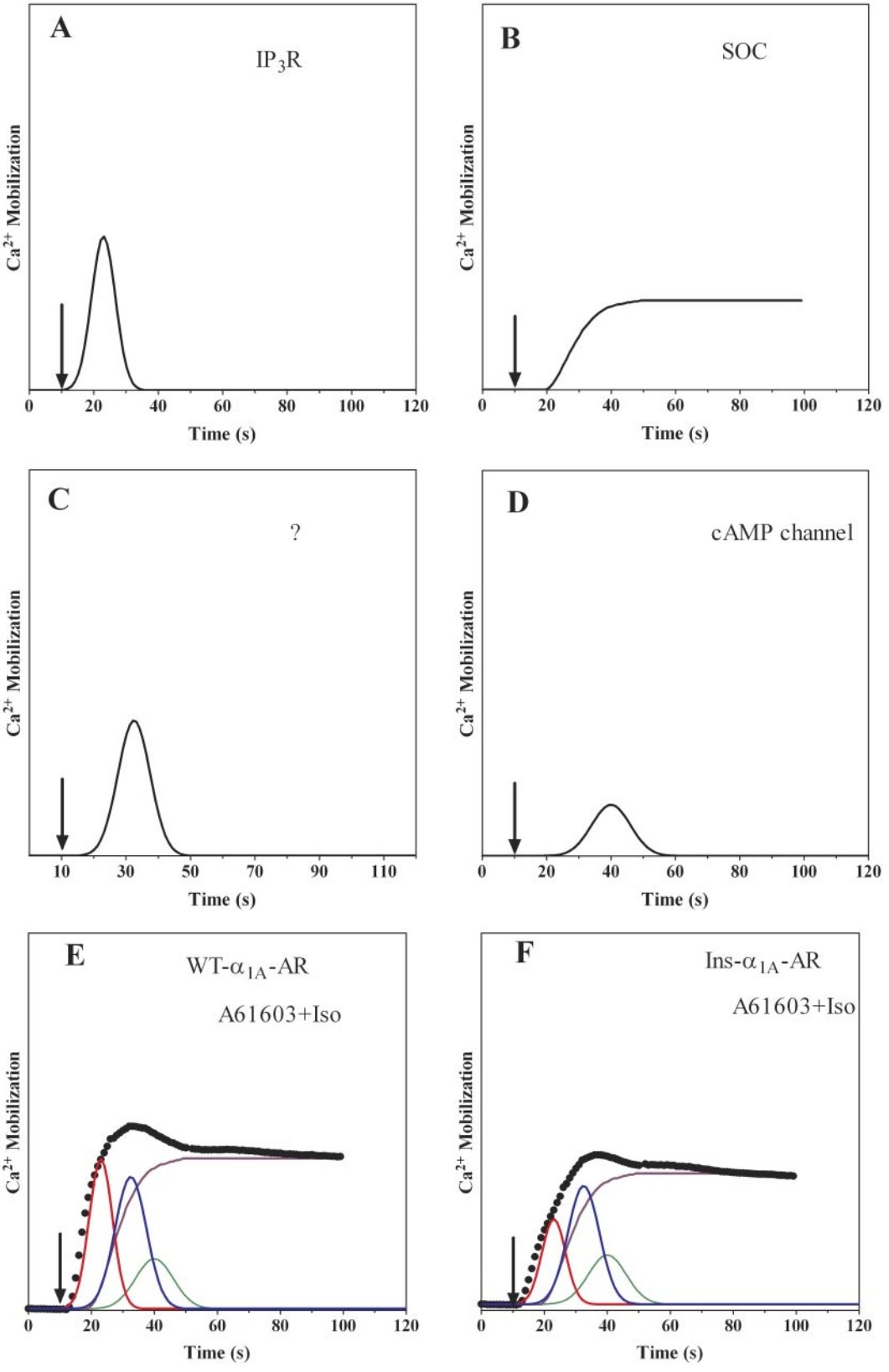

Fig. 8. Deconvolution of the hypothetical kinetic components of the calcium signaling response initiated by α_{1A}- and β_2-adrenoreceptors in HEK-293/EBNA cells. A, α_{1A}-AR-initiated Ca^{2+} mobilization in response to activation of endoplasmic reticulum IP_3 receptors (maximum at 12 s after agonist addition). B, α_{1A}-AR-initiated, sustained Ca^{2+} entry, probably a result of the opening of store-operated channels. C, α_{1A}-AR-initiated Ca^{2+} mobilization in response to an unidentified signaling event (maximum signal at 23 s). D, β_2-AR initiated, cAMP-dependent Ca^{2+} mobilization, reaching a maximum at around 30 s. E and F, depict the interplay of the fast (red), intermediate (blue), β_2-AR initiated (green), and sustained (violet) components leading to the observed Ca^{2+} transients in wild-type (E) and Ins_α_{1A}-AR (F), upon costimulation with A61603 and isoproterenol. The black symbols (●) are actual traces observed with wild-type (E) or Ins_α_{1A}-AR (F) upon stimulation with A61603 plus isoproterenol. The arrows indicate the point of agonist addition.

Our data show that β_2-AR activation can selectively influence the phases of α_{1A}-AR induced Ca^{2+} mobilization without affecting the rates of IP accumulation. Coactivation of β_2-AR, of adenylyl cyclase with forskolin, or stimulation of the G_s-coupled adenosine 2B receptor with NECA has no effect on the first, rapid phase reflecting release of Ca^{2+} via IP_3R. Thus, it seems that an elevation in intracellular cAMP has no bearing on the activity of phospholipase C and/or IP_3R. On the other hand, the sustained phase seemed to be uniformly potentiated by all three activation means, indicating a single mechanism for agonist-evoked calcium re-entry, either through capacitive Ca^{2+} release activated channels, diacylglycerol-activated transient receptor potential channels, or through noncapacitive arachidonic acid-activated calcium channels (Bugaj et al., 2005; Mignen et al., 2005; Martin and Cooper, 2006). The activity of the latter channel can be modulated via PKA phosphorylation mediated by A-kinase anchoring protein (Mignen et al., 2005).

We were surprised that removal of the fast transient and slow sustained phases of Ca^{2+} mobilization in response to α_{1A}-AR agonists, by application of selective blockers of the endoplasmic reticulum IP_3R and the plasma membrane SOCs, unmasked a distinct third phase. It could be argued that addition of xestospongin C simply delayed the IP_3-generated Ca^{2+} response. Thus, the third phase represents incomplete inhibition of IP_3R. Should that be the case, lower concentrations of xestospongin C would be expected to cause a lesser delay in Ca^{2+} mobilization. To address that possibility, we repeated this experiment at a lower concentration of xestospongin C and found that not to be the case; instead, the third phase remained insensitive to this IP_3R inhibitor, whereas the rapid Ca^{2+} mobilization phase reappeared but at lower amplitude (data not shown). Therefore, instead of observing a single response phase with intermediate kinetics, we observed the two distinct and well resolved phases, illustrated in Fig. 8, A and C.

We do not know at present the identity of the channel responsible for the third phase (Fig. 8C) or the signaling cascade leading to its activation. In preliminary studies both adenylyl cyclase and PKA inhibitors fully blocked all responses, indicating the additional phase is also affected by cAMP signaling (data not shown). We also found that pretreatment with thapsigargin, a sarco/endoplasmic reticulum Ca^{2+}-ATPase blocker, abolished all signals (data not shown). Therefore, the endoplasmic reticulum seems to be the likely source of Ca^{2+}. An alternate mechanism for the control of Ca^{2+} release from the endoplasmic reticulum involves ryanodine receptors. They have been shown to exist in several nonexcitable cell lines, although their functional expression in HEK-293 cells is controversial. RT-PCR analysis of HEK-293/EBNA cells found that significant levels of ryanodine receptor 2 mRNA are present in these cells.

Both coupling-deficient mutants are strongly potentiated by coactivation of β_2-AR. The Ins_α_{1A}-AR mutant showed significantly higher potentiation relative to the wild-type receptor. This may indicate that the coactivation of wild-type α_{1A}-AR with β_2-AR maximized the capacity for Ca^{2+} mobilization in those cells (response ceiling or saturation). Because the defective Ins_α_{1A}-AR mutant triggered a smaller increase in cytoplasmic Ca^{2+}, it likely allowed for greater potentiation by β_2-AR. Alternatively, higher concentrations of second messengers generated upon initial α_{1A}-AR activation may interfere with the β_2-AR mediated potentiation effect. Either way, our findings suggest that in native tissues, β_2-AR may act as an amplifier of α_{1A}-AR responses at "low" α_{1A}-AR functional settings.

The most striking result was observed with the G_q-uncoupled Sub_α_{1A}-AR mutant. Stimulation of cells expressing this variant with the α_{1A}-selective agonist A61603 yielded no detectable Ca^{2+} mobilization or IP generation, yet this mutant showed recovery of Ca^{2+} mobilization in response to costimulation with the β_2-AR agonist isoproterenol and the α_{1A}-AR agonist A61603. In those cells, A61603 increased β_2-AR activated Ca^{2+} mobilization in a concentration-dependent manner with an EC_{50} value consistent with the well documented activity of this compound at α_{1A}-AR. These observations may indeed imply the formation of α_{1A}/β_2-AR heterodimers in transduced cells, although additional studies will be necessary to confirm this. Trans-activation, one of the proposed mechanisms of action for allosteric activation of GPCR heterodimers, provides a straightforward interpretation for the obtained results (Carrillo et al., 2003; Milligan and Smith, 2007).

An alternate interpretation not invoking heterodimers can also be put forward. α_1-ARs have been found to activate multiple signaling pathways and to induce the generation of various second messengers depending on the agonist and cell line or tissue tested (reviewed in Perez, 2005). Still, little is known about the structural elements of the receptor involved in conferring functional selectivity, or the identity of any partner proteins. Thus, it is possible that the Sub_α_{1A} AR, even though uncoupled from G_q, may remain competent for induction of other signaling events that we have not probed. Moreover, activation of non-G_q signaling cascades may remain subject to regulation of the Sub_α_{1A}-AR cross-talk with β_2-AR. This would account for the observed increases in β_2-AR induced Ca^{2+}-mobilization on costimulation in Sub_α_{1A}-AR cells. Another interpretation involves β_2-AR mediated sensitization of α_{1A}-AR signaling; such a sensitizing effect might be revealed more clearly in the functionally impaired α_{1A}-AR variants. Although these alternative explanations remain plausible, the recovery of function observed with Sub_α_{1A}-AR cells upon costimulation with A61603 and isoproterenol would seem to favor the α_{1A}/β_2-AR heterodimer model.

Convergent regulation of Ca^{2+} channels involved in agonist-mediated Ca^{2+} mobilization provides another point of pathway intersection (Zamponi and Snutch, 2002). Multiple lines of evidence indicate that channel activity can be modulated by a variety of mechanisms, including 1) phosphorylation by protein kinase C, PKA, ERK, and other kinases (Martin et al., 2006; Schulz et al., 2008), 2) modulation by interacting proteins such as calmodulin, A-kinase anchoring protein, Snapin, G proteins ($\beta\gamma$ subunits), or even receptors themselves (e.g., β_2-AR with the L-type Ca^{2+} channel) (Davare et al., 2001; Mignen et al., 2005; Catterall et al., 2006; Suzuki et al., 2007) and 3) small molecule effectors (cAMP, cyclic ADP ribose, IP_3, arachidonic acid, diacylglycerol, etc.) (Hofmann et al., 1999; Berridge et al., 2003; Mignen et al., 2005; Higashida et al., 2007). Thus, coactivation of two cascades may lead to multiple effects converging on Ca^{2+} mobilization.

HEK-293 cells express markers common to cells of the neuronal lineage, including a wide variety of ligand- and

voltage-gated calcium channels (Shaw et al., 2002). For several of them, evidence of their expression includes electrophysiology studies as well as protein and mRNA measures (Berjukow et al., 1996; Mignen et al., 2005). The more extensively studied voltage-gated Ca_V channels, such as the L-type and N-type, have been shown to be subject to phosphorylation by PKA and protein kinase C (Kamp and Hell, 2000; Catterall et al., 2006), whereas several putative phosphorylation sites have been identified in the T-type channels (Talavera and Nilius, 2006). It is noteworthy that β-adrenergic stimulation is one known mechanism of facilitation of the T-type currents. More recently, Ca_v channels have been reported to be regulated by the mitogen-activated protein kinase signaling cascade via ERK. Although ERK-dependent enhancement of Ca_v currents is often due to up-regulation of the expression of these channels, the neuronal N-type channel may be ERK-phosphorylated and tonically stimulated by MAP kinases (Fitzgerald, 2002; Martin et al., 2006; Woodall et al., 2008). Therefore, activation of α_{1A}- and β_2-ARs could lead to simultaneous regulation of Ca_v via different mechanism, as has been demonstrated in cardiomyocytes expressing L-type channels (for review, see Kamp and Hell, 2000).

The expression of the α_{1A}- and β_2-ARs in myocardial tissue and their functional balance has been linked to the pathogenesis and progression of heart failure, implicating maladaption of adrenoceptor signaling (Huang et al., 2007; Feldman et al., 2008; Woodcock et al., 2008). The development of heart failure in humans is accompanied by an increase in catecholamine levels and a decrease in density and signaling of the predominant adrenoceptor in the healthy heart, β_1-AR (Lohse et al., 2003), with no changes in the levels of expression of β_2-AR (Feldman et al., 2008; Woodcock et al., 2008). Because α_{1A}-AR expression is maintained in heart failure, and the natural ligand norepinephrine is shared by both α- and β-adrenoceptors, α_{1A}- and β_2-ARs are suggested to play greater roles in maintaining cardiac performance in failing hearts (Brodde, 1991; Skomedal et al., 1997; Woodcock et al., 2008).

Multiple lines of preclinical and clinical evidence suggest that a balance between β- and α_1-AR signaling is critical for cardiomyocyte function and survival and may not necessarily involve the canonical pathways. In a transgenic mouse model, over-expression of G_q induces cardiac hypertrophy, loss of β-AR inotropic responsiveness (D'Angelo et al., 1997), and ultimately leads to heart failure (Sakata et al., 1998). On the other hand, α_{1A}/α_{1B} double-knockout mice also developed heart failure after transverse aortic constriction and reconstitution of α_{1A} signaling in cardiomyocytes from those animals rescued them from NE-induced apoptosis (O'Connell et al., 2006). The expected IP generation was not detectable on those cardiomyocytes with reconstituted α_{1A}-AR function or in wild-type mouse cardiomyocytes, pointing at a non-G_q signaling mode for this receptor in myocardial function. Huang et al. (2007) reported that α_{1A}-AR stimulation of an ERK-mediated pathway is critical for cardiomyocyte survival.

Seemingly contradicting clinical trial outcomes can actually be reconciled through this concept of α_1/β-AR balanced pharmacology in the heart: although the selective α_1-AR antagonist doxazosin worsened heart failure symptoms and increased mortality in patients with heart failure, the nonselective antagonist carvedilol has shown efficacious in the treatment of this condition and it is perhaps the most efficacious β-blocker in the clinic (ALLHAT, 2000; Metra et al., 2000). Thus, identifying the functional relationships between β_2- and α_{1A}-ARs may be critical for understanding the pathophysiology of the failing heart and for identifying further therapies.

Toward that goal, we have studied the cross-talk between α_{1A}- and β_2-AR pathways employing a real-time functional measure combined with pharmacological analysis. Receptor cross-talk remains challenging to study at the cellular level, and native cellular models often display undetectable or altered receptor function, as a result of cell isolation and culturing before experimentation. On the other hand, studies employing systems relying on recombinant receptor expression commonly suffer from receptor overproduction, leading to experimental artifacts. Thus, our approach was to take advantage of the well characterized HEK-293 cell line, which endogenously expresses β_2-AR, by introducing α_{1A}-AR at low, and thus more physiological, expression levels. We employed the nonselective histone deacetylase inhibitor sodium butyrate to fine-tune receptor expression to levels comparable with the ones observed in native adrenergic tissues, as measured by radioligand binding. This system allowed us to measure real-time adrenoceptor signaling via Ca^{2+} measurements derived from single or combined α_{1A}- and β_2-AR activation. Our data provide for the first time detailed information on bidirectional cross-talk between α_{1A} and β_2 adrenoceptors. Surprisingly, these data indicate that their functional interaction involves either heterodimer formation and/or the presence of yet to be identified G_q or non-G_q signaling events in response to α_{1A}-AR activation. Neither of those possibilities has been considered before to account for the physiological observations suggesting cross-talk between these two receptors. Dissection of the precise interplay of those signaling pathways in normal and diseased heart tissue, and in response to pharmacological agents, is the obvious follow-up to our studies. Such future study offers great potential for developing safer and more efficacious drugs for the treatment of heart failure and related conditions.

Acknowledgments

We are grateful to the Discovery Technologies Group of Roche Palo Alto: Michelle Browner and Tom Novak for their critical support to enable this work, and Pamela Olson, Simon Lee, Mariola Ilnicka, and Nixy Zutshi for help or expert advice. We also thank members of the In Vitro Pharmacology Group-Inflammation Discovery.

References

ALLHAT (2000) Major cardiovascular events in hypertensive patients randomized to doxazosin vs chlorthalidone: the antihypertensive and lipid-lowering treatment to prevent heart attack trial (ALLHAT). ALLHAT Collaborative Research Group. *JAMA* **283:**1967–1975.

Berjukow S, Döring F, Froschmayr M, Grabner M, Glossmann H, and Hering S (1996) Endogenous calcium channels in human embryonic kidney (HEK293) cells. *Br J Pharmacol* **118:**748–754.

Berridge MJ, Bootman MD, and Roderick HL (2003) Calcium signalling: dynamics, homeostasis and remodelling. *Nat Rev Mol Cell Biol* **4:**517–529.

Boffa LC, Vidali G, Mann RS, and Allfrey VG (1978) Suppression of histone deacetylation in vivo and in vitro by sodium butyrate. *J Biol Chem* **253:**3364–3366.

Brodde OE (1991) Beta 1- and beta 2-adrenoceptors in the human heart: properties, function, and alterations in chronic heart failure. *Pharmacol Rev* **43:**203–242.

Bugaj V, Alexeenko V, Zubov A, Glushankova L, Nikolaev A, Wang Z, Kaznacheyeva E, Bezprozvanny I, and Mozhayeva GN (2005) Functional properties of endogenous receptor- and store-operated calcium influx channels in HEK293 cells. *J Biol Chem* **280:**16790–16797.

Carrillo JJ, Pediani J, and Milligan G (2003) Dimers of class A G protein-coupled receptors function via agonist-mediated trans-activation of associated G proteins. *J Biol Chem* **278:**42578–42587.

Catterall WA, Hulme JT, Jiang X, and Few WP (2006) Regulation of sodium and

calcium channels by signaling complexes. *J Recept Signal Transduct Res* **26:**577–598.
Cheng Y and Prusoff WH (1973) Relationship between the inhibition constant (K1) and the concentration of inhibitor which causes 50 per cent inhibition (I50) of an enzymatic reaction. *Biochem Pharmacol* **22:**3099–3108.
Clapham DE (2007) Calcium signaling. *Cell* **131:**1047–1058.
Cooper J, Hill SJ, and Alexander SP (1997) An endogenous A2B adenosine receptor coupled to cyclic AMP generation in human embryonic kidney (HEK 293) cells. *Br J Pharmacol* **122:**546–550.
Cordeaux Y and Hill SJ (2002) Mechanisms of cross-talk between G-protein-coupled receptors. *Neuro-Signals* **11:**45–57.
Cotecchia S, Exum S, Caron MG, and Lefkowitz RJ (1990) Regions of the alpha 1-adrenergic receptor involved in coupling to phosphatidylinositol hydrolysis and enhanced sensitivity of biological function. *Proc Natl Acad Sci U S A* **87:**2896–2900.
D'Angelo DD, Sakata Y, Lorenz JN, Boivin GP, Walsh RA, Liggett SB, and Dorn GW 2nd (1997) Transgenic Galphaq overexpression induces cardiac contractile failure in mice. *Proc Natl Acad Sci U S A* **94:**8121–8126.
Davare MA, Avdonin V, Hall DD, Peden EM, Burette A, Weinberg RJ, Horne MC, Hoshi T, and Hell JW (2001) A beta2 adrenergic receptor signaling complex assembled with the Ca^{2+} channel Cav1.2. *Science* **293:**98–101.
Dzimiri N (2002) Receptor crosstalk: implications for cardiovascular function, disease and therapy. *Eur J Biochem* **269:**4713–4730.
Feldman DS, Elton TS, Sun B, Martin MM, and Ziolo MT (2008) Mechanisms of disease: detrimental adrenergic signaling in acute decompensated heart failure. *Nat Clin Pract Cardiovasc Med* **5:**208–218.
Fitzgerald EM (2002) The presence of Ca^{2+} channel beta subunit is required for mitogen-activated protein kinase (MAPK)-dependent modulation of alpha1B Ca^{2+} channels in COS-7 cells. *J Physiol* **543:**425–437.
Ford AP, Daniels DV, Chang DJ, Gever JR, Jasper JR, Lesnick JD, and Clarke DE (1997) Pharmacological pleiotropism of the human recombinant alpha1A-adrenoceptor: implications for alpha1-adrenoceptor classification. *Br J Pharmacol* **121:**1127–1135.
Gilchrist A (2007) Modulating G-protein-coupled receptors: from traditional pharmacology to allosterics. *Trends Pharmacol Sci* **28:**431–437.
Greasley PJ, Fanelli F, Scheer A, Abuin L, Nenniger-Tosato M, DeBenedetti PG, and Cotecchia S (2001) Mutational and computational analysis of the alpha(1b)-adrenergic receptor. Involvement of basic and hydrophobic residues in receptor activation and G protein coupling. *J Biol Chem* **276:**46485–46494.
Higashida H, Salmina AB, Olovyannikova RY, Hashii M, Yokoyama S, Koizumi K, Jin D, Liu HX, Lopatina O, Amina S, et al. (2007) Cyclic ADP-ribose as a universal calcium signal molecule in the nervous system. *Neurochem Int* **51:**192–199.
Hoffmann C, Gaietta G, Bünemann M, Adams SR, Oberdorff-Maass S, Behr B, Vilardaga JP, Tsien RY, Ellisman MH, and Lohse MJ (2005) A FlAsH-based FRET approach to determine G protein-coupled receptor activation in living cells. *Nat Methods* **2:**171–176.
Hofmann T, Obukhov AG, Schaefer M, Harteneck C, Gudermann T, and Schultz G. (1999) Direct activation of human TRPC6 and TRPC3 channels by diacylglycerol. *Nature* **397:**259–263.
Huang Y, Wright CD, Merkwan CL, Baye NL, Liang Q, Simpson PC, and O'Connell TD (2007) An alpha1A-adrenergic-extracellular signal-regulated kinase survival signaling pathway in cardiac myocytes. *Circulation* **115:**763–772.
Hur EM and Kim KT (2002) G protein-coupled receptor signalling and cross-talk: achieving rapidity and specificity. *Cell Signalling* **14:**397–405.
Kamp TJ and Hell JW (2000) Regulation of cardiac L-type calcium channels by protein kinase A and protein kinase C. *Circ Res* **87:**1095–1102.
Kenakin TP (2004) *A Pharmacology Primer: Theory, Application and Methods.* Elsevier, Amsterdam.
Lohse MJ, Engelhardt S, and Eschenhagen T (2003) What is the role of beta-adrenergic signaling in heart failure?. *Circ Res* **93:**896–906.
Lohse MJ, Hein P, Hoffmann C, Nikolaev VO, Vilardaga JP, and Bunemann M (2008a) Kinetics of G-protein-coupled receptor signals in intact cells. *Br J Pharmacol* **153:**S125–S132.
Lohse MJ, Nikolaev VO, Hein P, Hoffmann C, Vilardaga JP, and Bunemann M (2008b) Optical techniques to analyze real-time activation and signaling of G-protein-coupled receptors. *Trends Pharmacol Sci* **29:**159–165.
Martin AC and Cooper DM (2006) Capacitative and 1-oleyl-2-acetyl-sn-glycerol-activated Ca^{2+} entry distinguished using adenylyl cyclase type 8. *Mol Pharmacol* **70:**769–777.
Martin SW, Butcher AJ, Berrow NS, Richards MW, Paddon RE, Turner DJ, Dolphin AC, Sihra TS, and Fitzgerald EM (2006) Phosphorylation sites on calcium channel alpha1 and beta subunits regulate ERK-dependent modulation of neuronal N-type calcium channels. *Cell Calcium* **39:**275–292.
Metra M, Giubbini R, Nodari S, Boldi E, Modena MG, and Dei Cas L (2000) Differential effects of beta-blockers in patients with heart failure: A prospective, randomized, double-blind comparison of the long-term effects of metoprolol versus carvedilol. *Circulation* **102:**546–551.
Mignen O, Thompson JL, and Shuttleworth TJ (2005) Arachidonate-regulated Ca^{2+}-selective (ARC) channel activity is modulated by phosphorylation and involves an A-kinase anchoring protein. *J Physiol* **567:**787–798.
Milligan G and Smith NJ (2007) Allosteric modulation of heterodimeric G-protein-coupled receptors. *Trends Pharmacol Sci* **28:**615–620.
Minneman KP (1988) Alpha 1-adrenergic receptor subtypes, inositol phosphates, and sources of cell Ca^{2+}. *Pharmacol Rev* **40:**87–119.
O'Connell TD, Swigart PM, Rodrigo MC, Ishizaka S, Joho S, Turnbull L, Tecott LH, Baker AJ, Foster E, Grossman W, et al. (2006) Alpha1-adrenergic receptors prevent a maladaptive cardiac response to pressure overload. *J Clin Investig* **116:**1005–1015.
Oldham WM and Hamm HE (2007) How do receptors activate G proteins?. *Adv Protein Chem* **74:**67–93.
Perez DM (2005) *The Adrenergic Receptors: In the 21st Century.* Humana Press, Totowa, NJ.
Perez DM (2007) Structure-function of alpha1-adrenergic receptors. *Biochem Pharmacol* **73:**1051–1062.
Prinster SC, Hague C, and Hall RA (2005) Heterodimerization of g protein-coupled receptors: specificity and functional significance. *Pharmacol Rev* **57:**289–298.
Sakata Y, Hoit BD, Liggett SB, Walsh RA, and Dorn GW 2nd (1998) Decompensation of pressure-overload hypertrophy in G alpha q-overexpressing mice. *Circulation* **97:**1488–1495.
Schulz DJ, Temporal S, Barry DM, and Garcia ML (2008) Mechanisms of voltage-gated ion channel regulation: from gene expression to localization. *Cell Mol Life Sci* **65:**2215–2231.
Shaw G, Morse S, Ararat M, and Graham FL (2002) Preferential transformation of human neuronal cells by human adenoviruses and the origin of HEK 293 cells. *FASEB J* **16:**869–871.
Skomedal T, Borthne K, Aass H, Geiran O, and Osnes JB (1997) Comparison between alpha-1 adrenoceptor-mediated and beta adrenoceptor-mediated inotropic components elicited by norepinephrine in failing human ventricular muscle. *J Pharmacol Exp Ther* **280:**721–729.
Suzuki F, Morishima S, Tanaka T, and Muramatsu I (2007) Snapin, a new regulator of receptor signaling, augments alpha1A-adrenoceptor-operated calcium influx through TRPC6. *J Biol Chem* **282:**29563–29573.
Talavera K and Nilius B (2006) Biophysics and structure-function relationship of T-type Ca^{2+} channels. *Cell Calcium* **40:**97–114.
Violin JD, DiPilato LM, Yildirim N, Elston TC, Zhang J, and Lefkowitz RJ (2008) beta2-adrenergic receptor signaling and desensitization elucidated by quantitative modeling of real time cAMP dynamics. *J Biol Chem* **283:**2949–2961.
Violin JD and Lefkowitz RJ (2007) Beta-arrestin-biased ligands at seven-transmembrane receptors. *Trends Pharmacol Sci* **28:**416–422.
Waugh DJ, Gaivin RJ, Damron DS, Murray PA, and Perez DM (1999) Binding, partial agonism, and potentiation of alpha(1)-adrenergic receptor function by benzodiazepines: A potential site of allosteric modulation. *J Pharmacol Exp Ther* **291:**1164–1171.
Werry TD, Wilkinson GF, and Willars GB (2003) Mechanisms of cross-talk between G-protein-coupled receptors resulting in enhanced release of intracellular Ca^{2+}. *Biochem J* **374:**281–296.
Williams TJ, Blue DR, Daniels DV, Davis B, Elworthy T, Gever JR, Kava MS, Morgans D, Padilla F, Tassa S, et al. (1999) In vitro alpha1-adrenoceptor pharmacology of Ro 70-0004 and RS-100329, novel alpha1A-adrenoceptor selective antagonists. *Br J Pharmacol* **127:**252–258.
Woodall AJ, Richards MA, Turner DJ, and Fitzgerald EM (2008) Growth factors differentially regulate neuronal Cav channels via ERK-dependent signalling. *Cell Calcium* **43:**562–575.
Woodcock EA, Du XJ, Reichelt ME, and Graham RM (2008) Cardiac alpha 1-adrenergic drive in pathological remodelling. *Cardiovasc Res* **77:**452–462.
Zamponi GW and Snutch TP (2002) Modulating modulation: crosstalk between regulatory pathways of presynaptic calcium channels. *Mol Interv* **2:**476–478.

Address correspondence to: Marcos E. Milla, 3431 Hillview Avenue, Mailstop R2–101, Palo Alto, CA 94304. E-mail: marcos.milla@roche.com